



This is to certify that the

thesis entitled

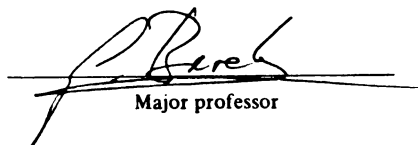
EFFECTS OF AMBIENT CONDITIONS ON THE
EMISSIONS OF A SMALL CARBURETED OVERHEAD
VALVE FOUR STROKE UTILITY ENGINE

presented by

Erik C. Bertrand

has been accepted towards fulfillment
of the requirements for

M.S. degree in Mechanical Engineering


Major professor

Date August 14, 1997



PLACE IN RETURN BOX
to remove this checkout from your record.
TO AVOID FINES return on or before date due.

| DATE DUE | DATE DUE | DATE DUE |
|----------------------|----------------|----------------|
| 0 9 1 5 1 4 _____ | _____ _____ | _____ _____ |
| _____ _____ | _____ _____ | _____ _____ |
| _____ _____ | _____ _____ | _____ _____ |
| _____ _____ | _____ _____ | _____ _____ |
| _____ _____ | _____ _____ | _____ _____ |

**EFFECTS OF AMBIENT CONDITIONS ON THE EMISSIONS OF A SMALL
CARBURETED OVERHEAD VALVE FOUR STROKE UTILITY ENGINE**

By

Erik C. Bertrand

A THESIS

Submitted to
Michigan State University
in partial fulfillment of the requirements
for the degree of

MASTER OF SCIENCE

Department of Mechanical Engineering

1997

ABSTRACT

EFFECTS OF AMBIENT CONDITIONS ON THE EMISSIONS OF A SMALL CARBURETED OVERHEAD VALVE FOUR STROKE UTILITY ENGINE

By

Erik C. Bertrand

Small hand-held utility engines are increasingly becoming a factor in emissions production and regulation. This paper outlines a laboratory study of the effects of ambient conditions on the steady state emissions and performance of a typical air-cooled, overhead valve, carbureted, single cylinder four-stroke engine used for lawn and garden applications. In this study, the ambient temperature and relative humidity (and thus specific humidity) were thermostatically controlled, with one varied while the other was held nearly constant. The engine testing was performed at *WOT* under steady-state conditions at a fixed engine speed using a hydraulic dynamometer.

Experimental results show that in carbureted engines, the main effect of changes in ambient conditions is to change the intake air properties and therefore the metered air/fuel ratio (*AFR*). Moderate changes in ambient conditions lead to small changes in the *AFR* but large changes in emissions output. Definite trends existed in the air-fuel ratio, engine torque, *CO*, *CO*₂, *NO*_x emissions, as the ambient conditions were varied. For example, a 0.009 decrease (0.015 to 0.006) in the specific humidity resulted in a 50% reduction in *NO*_x emissions.

ACKNOWLEDGMENTS

I have a few important people I would like to thank:

Dr. Giles Brereton, my advisor, for his guidance, intuition and ambition. Without his help graduate school would have been much more difficult, if not unlikely. Dr. Harold Schock, for giving me the chance to become associated with the MSU Engine Research lab. My wife, Nancy, for sticking by me throughout the latter part of my undergraduate education and graduate school, despite the lack of attention. My father, Marc, for his financial and educational input. Without his advice, it would not have been possible to attend undergraduate or graduate school. My mother, Kathy, whose good spirit and positive thinking made an overwhelming task seem almost effortless. Tom Stuecken for the countless brackets, fixtures and components that were fabricated along with the relentless pursuit of perfection. My Grandfather, although no longer on this earth, would have been proud. Lastly, I would like to thank the Environmental Protection Agency, Ann Arbor, Michigan for supporting this work.

TABLE OF CONTENTS

| | |
|--|-----|
| ACKNOWLEDGMENTS..... | iii |
| TABLE OF CONTENTS | iv |
| LIST OF TABLES | vi |
| LIST OF FIGURES | vii |
| NOMENCLATURE..... | ix |
| 1. INTRODUCTION..... | 1 |
| 1.1 Overview | 1 |
| 1.2 Four Stroke Operation..... | 3 |
| 1.3 Emission Characteristics of Small O.H.V. Four Stroke Engines | 5 |
| 1.3.1 Emissions from rich air / fuel ratios | 5 |
| 1.3.2 Emissions from high temperature combustion..... | 6 |
| 1.4 Literature Review | 6 |
| 1.5 Objectives..... | 10 |
| 2. EXPERIMENTAL METHODS | 12 |
| 2.1 The Test Engine | 12 |
| 2.2 Climate Control | 12 |
| 2.3 Experimental Apparatus..... | 13 |
| 2.4 Experimental Procedure | 14 |
| 2.4.1 Measured Quantities..... | 15 |
| 2.4.2 Calibration..... | 15 |
| 2.4.3 Temperature Variation | 17 |
| 2.4.4 Humidity Variation..... | 17 |
| 3. RESULTS..... | 18 |

| | |
|---------------------------------------|----|
| 3.1 Theoretical Equations..... | 18 |
| 3.1.1 Carburation..... | 18 |
| 3.1.2 Compression..... | 25 |
| 3.1.3 Combustion | 28 |
| 3.2 Theoretical Results..... | 29 |
| 3.3 Experimental Results | 35 |
| 3.3.1 Humidity Variation..... | 35 |
| 3.3.2 Temperature Variation | 43 |
| 4. CONCLUSIONS | 51 |
| Appendix A | 53 |
| A.1 Fuel Flow Measurement..... | 53 |
| A.2 Dynamometer and Controls..... | 55 |
| A.3 Environmental Controls | 57 |
| A.4 Dilution Tunnel | 58 |
| A.5 Emission Measurement | 59 |
| A.6 Data Collection..... | 62 |
| Appendix B | 64 |
| B.1 Heat Transfer | 65 |
| B.2 Work | 66 |
| B.3 Internal Energy..... | 68 |
| B.4 Change in Gibbs Free Energy | 68 |
| Appendix C | 70 |
| Appendix D | 72 |
| Appendix E..... | 75 |
| LIST OF REFERENCES | 76 |

LIST OF TABLES

| | |
|--|-----------|
| TABLE 1: CARB EXHAUST EMISSION STANDARDS..... | 3 |
| TABLE 2: BASIC FOUR STROKE OPERATION..... | 3 |
| TABLE 3: CALIFORNIA CURRENT EMISSION STANDARDS..... | 10 |
| TABLE 4: THE TEST ENGINE..... | 12 |
| TABLE 5: EQUIPMENT USED..... | 13 |
| TABLE 6: EMISSION MEASUREMENT TECHNIQUES..... | 62 |
| TABLE 7: TABLE OF WOSHNI COEFFICIENTS..... | 65 |

LIST OF FIGURES

| | |
|---|----|
| FIGURE 1: COMPOSITION OF EXHAUST AND FUEL AS A FUNCTION OF CARBON NUMBER [6] | 8 |
| FIGURE 2: EXHAUST EMISSION SOURCES [4] | 8 |
| FIGURE 3: OVERVIEW OF TEST CELL..... | 14 |
| FIGURE 4: CROSS SECTION OF CARBURETOR THROAT..... | 19 |
| FIGURE 5: PRESSURE - VOLUME DIAGRAM | 27 |
| FIGURE 6: ACTUAL <i>AFR</i> VS. DESIGN <i>AFR</i> | 30 |
| FIGURE 7: COMBUSTION TEMPERATURE VS. ACTUAL <i>AFR</i> | 30 |
| FIGURE 8: COMBUSTION TEMPERATURE VS. DESIGN <i>AFR</i> | 31 |
| FIGURE 9: ACTUAL <i>AFR</i> VS. DESIGN <i>AFR</i> | 32 |
| FIGURE 10: PEAK COMBUSTION TEMPERATURE VS. ACTUAL <i>AFR</i> | 33 |
| FIGURE 11: PEAK COMBUSTION TEMPERATURE VS. DESIGN <i>AFR</i> | 33 |
| FIGURE 12: CO/CO ₂ RATIO VS. DESIGN <i>AFR</i> (1) | 34 |
| FIGURE 13: CO/CO ₂ RATIO VS. DESIGN <i>AFR</i> (2) | 34 |
| FIGURE 14: ROOM TEMPERATURE VS. SPECIFIC HUMIDITY | 36 |
| FIGURE 15: ENGINE TORQUE VS. SPECIFIC HUMIDITY | 37 |
| FIGURE 16: BSFC VS. SPECIFIC HUMIDITY..... | 38 |
| FIGURE 17: CO VS. SPECIFIC HUMIDITY | 39 |
| FIGURE 18: CO ₂ VS. SPECIFIC HUMIDITY | 39 |
| FIGURE 19: NO _x VS. SPECIFIC HUMIDITY | 40 |
| FIGURE 20: HC VS. SPECIFIC HUMIDITY | 41 |

| | |
|--|----|
| FIGURE 21: <i>AFR</i> VS. SPECIFIC HUMIDITY | 42 |
| FIGURE 22: CO/CO ₂ RATIO VS. SPECIFIC HUMIDITY | 42 |
| FIGURE 23: SPECIFIC HUMIDITY VS. ROOM TEMPERATURE | 44 |
| FIGURE 24: ENGINE TORQUE VS. ROOM TEMPERATURE | 45 |
| FIGURE 25: BSFC VS. ROOM TEMPERATURE | 45 |
| FIGURE 26: CO VS. ROOM TEMPERATURE..... | 46 |
| FIGURE 27: CO ₂ VS. ROOM TEMPERATURE..... | 47 |
| FIGURE 28: NOX VS. ROOM TEMPERATURE..... | 47 |
| FIGURE 29: HC VS. ROOM TEMPERATURE..... | 48 |
| FIGURE 30: <i>AFR</i> VS. ROOM TEMPERATURE..... | 49 |
| FIGURE 31: CO/CO ₂ RATIO VS. ROOM TEMPERATURE..... | 50 |
| FIGURE 32: VIBRATING FLOW TUBE (SINGLE FLOW TUBE SHOWN) | 54 |
| FIGURE 33: FLUID FORCES REACTING IN VIBRATION OF FLOW TUBE | 54 |
| FIGURE 34: END VIEW OF FLOW TUBE SHOWING TWIST | 54 |
| FIGURE 35: FUEL FLOW CART..... | 55 |
| FIGURE 36: DYNAMOMETER HYDRAULIC CIRCUIT | 56 |
| FIGURE 37: TEMPERATURE AND HUMIDITY CONTROLS..... | 57 |
| FIGURE 38: DILLUTION TUNNEL | 59 |
| FIGURE 39: ANALYZER CROSS SECTIONS | 61 |
| FIGURE 40: DATA COLLECTING COMPUTER (486 PC) | 63 |
| FIGURE 41: DATA COLLECTING ALGORITHM..... | 63 |
| FIGURE 42: WORK INPUTS AND OUTPUTS..... | 66 |

NOMENCLATURE

English Symbols

| <u>Name</u> | <u>Meaning</u> | <u>Units</u> |
|-------------|-----------------------|--------------|
| a | Moles of Air | $kmoles$ |
| a_a | Moles of Air (actual) | $kmoles$ |
| a_d | Moles of Air (design) | $kmoles$ |
| b | Moles of Water Vapor | $kmoles$ |
| c | Speed of Sound | m/sec |
| \dot{m} | Mass Flow Rate | kg/sec |
| m_{air} | Mass of Air | kg |
| m_{fuel} | Mass of Fuel | kg |
| n_{air} | Moles of Air | $kmoles$ |

| | | |
|------------|------------------------------------|------------------------------|
| n_{fuel} | Moles of Fuel | <i>kmoles</i> |
| v | Specific Volume | <i>meters³/kg</i> |
| w | Moles of CO_2 | <i>kmoles</i> |
| x | Moles of CO | <i>kmoles</i> |
| y | Moles of HC | <i>kmoles</i> |
| z | Moles of NO_x | <i>kmoles</i> |
| C_v | Specific heat at constant volume | <i>kJ/kg - K</i> |
| C_p | Specific heat at constant pressure | <i>kJ/kg - K</i> |
| K_p | Equilibrium Constant | - |
| M | Molal Mass | <i>kg/kmole</i> |
| \hat{M} | Mach Number | <i>m/sec</i> |
| P_{REF} | Reference Pressure | <i>atm</i> |
| P | Pressure | <i>atm</i> |
| P_1 | Pressure at start of compression | <i>atm</i> |

| | | |
|-----------|-------------------------------------|-------------------------------|
| P_o | Reference Pressure | <i>atm</i> |
| \bar{R} | Universal gas constant | <i>kJ/kmol – K</i> |
| R_{MIX} | Specific gas constant | <i>kJ/kg – K</i> |
| T_{REF} | Reference Temperature | <i>K</i> |
| T | Temperature | <i>K</i> |
| T_1 | Temperature at start of compression | <i>K</i> |
| V | Volume | <i>meters³</i> |
| \dot{V} | Volume Flow Rate | <i>meters³/sec</i> |

Greek Symbols

| <u>Symbol</u> | <u>Meaning</u> | <u>Units</u> |
|---------------|-------------------|-------------------------------|
| ω | Specific Humidity | <i>kgH₂O/kgAIR</i> |
| ρ | Density | <i>kg/meter³</i> |

Acronyms

| <u>Symbol</u> | <u>Meaning</u> | <u>Units</u> |
|------------------------|--|---------------------|
| <i>AFR</i> | Air Fuel Ratio | <i>kgAIR/kgFUEL</i> |
| <i>AFR_a</i> | Actual Air Fuel Ratio | <i>kgAIR/kgFUEL</i> |
| <i>AFR_d</i> | Design Air Fuel Ratio | <i>kgAIR/kgFUEL</i> |
| <i>BSFC</i> | Brake Specific Fuel Consumption | <i>gr/kW - hr</i> |
| <i>CO</i> | Carbon Monoxide | - |
| <i>CO₂</i> | Carbon Dioxide | - |
| <i>HC</i> | Hydrocarbons | - |
| <i>NO_x</i> | Oxides of Nitrogen (<i>NO</i> and <i>NO₂</i>) | - |
| <i>OHV</i> | Over Head Valve | - |
| <i>WOT</i> | Wide Open Throttle | - |

1. INTRODUCTION

1.1 Overview

Internal combustion engines come in a variety of shapes, sizes and configurations. From tiny 1.6cc (.001638 liter) model aircraft engines to 434,257cc (434 liters) large ship powering diesels, they all have one thing in common: they use some type of fuel to do “useful” work for mankind. In addition there are many designs of internal combustion engines using mainly two types of fuel: gasoline and Diesel. Four stroke engines and their cousins the two stroke models are similar in many ways. For example, they both use a piston cylinder arrangement to compress the air / fuel mixture to some fraction of its original volume. Likewise, they can run on either gasoline or Diesel fuel, and can be liquid or air cooled. In a four stroke engine, the cylinder filling and emptying is controlled largely by the camshaft timing and the moving piston.

In a two stroke engine, the cylinder filling and emptying are controlled by the inlet and exhaust ports cast into the cylinder walls. The two stroke engine has no clear defining line between the four combustion events that happen in the four stroke engine. It is this lack of cylinder event definition that may lead to the decline of the two stroke engine, in the small engine / utility arena. Two stroke hydrocarbon emissions in exhaust gases are typically found to be at least ten times greater for similar engine displacements and power outputs. For many years, the automobile has been considered as one of the most serious polluters, powered by internal combustion engines. However this may no longer be true.

California Air Resources Board (CARB) studies found that two-cycle engines in California produce 48,000 kg per day of total exhaust hydrocarbons, and 150,000 kg per day of carbon monoxide [21]. Using these estimates, hydrocarbon and carbon monoxide emissions from utility engines in the state are equal to the emissions produced by 3.5 million new cars driven 26,000 km (16,000 miles).

CARB has since proposed standards to regulate emissions from several types of utility engines that are smaller than 225 cc and less than 19 kW (25 hp). These categories cover lawn and garden equipment and general utility equipment such as pumps, generators and compressors. The 1995 standards for lawn and garden equipment includes a category for hand-held engines with a displacement of 20 cc to 50 cc. These standards are 241 g/kW-hr Hydrocarbons (HC), 804 g/kW-hr Carbon Monoxide (CO), and 5.4 g/kW-hr Oxides of Nitrogen (NO_x). The 1999 standards are 67 g/kW-hr HC , 174 g/kW-hr CO , and 5.4 g/kW-hr NO_x . As a result of these new regulations, small engine manufacturers are required to reduce emission output from their engines, see Table 1.

It is important to understand the role ambient conditions play in evaluating emission output from these sources. As emission regulations for small engines are phased in, it will be important to specify the testing conditions under which regulations must be met. The test parameters include the ambient conditions (atmospheric pressure, air temperature and humidity) under which the test was carried out. It has been known for a long time that temperature and humidity affect engine performance and emission output [2]. In addition, the valid testing ranges of ambient conditions acceptable for measuring emission output, have not yet been set by CARB or the Environmental Protection Agency (EPA). It is for these reasons that this study has been undertaken; to better understand how ambient conditions affect emission output levels and to provide some insight as to appropriate ambient testing parameters.

Table 1: CARB Exhaust Emission Standards
(gr/brake kW-hr)

| YEAR | ENGINE CLASS | HC + NO _x | HC | NO _x | CO |
|-------|---|----------------------|-----|-----------------|-----|
| 1995 | I | 16.1 | - | - | 402 |
| | II | 13.4 | - | - | 402 |
| | III | - | 295 | 5.4 | 804 |
| | IV | - | 241 | 5.4 | 804 |
| | V | - | 161 | 5.4 | 402 |
| 1999 | I, II | 4.3 | - | - | 134 |
| | III, IV, V | - | 67 | 5.4 | 174 |
| CLASS | DESCRIPTION | | | | |
| I | Non hand held, less than 225cc displacement | | | | |
| II | Non hand held, greater or equal to 225cc displacement | | | | |
| III | Hand held, less than 20cc displacement | | | | |
| IV | Hand held, 20cc to less than 50cc displacement | | | | |
| V | Hand held, greater or equal to 50cc displacement | | | | |

1.2 Four Stroke Operation

Four stroke engines utilize four distinct processes for each combustion event and are summarized in table 2.

Table 2: Basic Four Stroke Operation

| EVENT | PISTON DIRECTION | ACTION | VALVE OPEN | |
|-------------|------------------|--|------------|---------|
| | | | INTAKE | EXHAUST |
| INTAKE | DOWN | FRESH CHARGE IS DRAWN INTO THE CYLINDER | X | |
| COMPRESSION | UP | THE MIXTURE IS COMPRESSED TO A FRACTION OF ITS ORIGINAL VOLUME | | |
| EXPANSION | DOWN | THE MIXTURE IS IGNITED PRODUCTS ARE PRODUCED | | |
| EXHAUST | UP | THE PRODUCTS ARE EXPELLED FROM THE CYLINDER | | X |

The first step in the process is the intake stroke. During this process, only the intake valve is open and the piston is moving down within the cylinder. This creates a

vacuum and draws air in past the carburetor, through the intake ports, around the intake valve and into the cylinder. Next, the intake valve closes and the piston starts to move upwards. This compresses the fuel / air mixture within the cylinder prior to ignition. The final pressure and temperature within the cylinder is a function of many things but most important are compression ratio, port design and mixture properties. When the piston is close to Top Dead Center (TDC), a spark is delivered to the spark plug initiating combustion within the cylinder. This combustion drastically increases the mixture temperature and therefore the pressure within the cylinder and thus forces the piston downward. When the piston is near Bottom Dead Center (BDC), the exhaust valve is opened allowing blowdown of the cylinder. Blowdown happens when the pressure inside the combustion cylinder is higher than the pressure within the exhaust manifold, thus allowing the newly created exhaust products to escape. The process is further helped along when the piston starts moving upward decreasing the volume within the cylinder and further forcing exhaust products out of the cylinder. Unlike a two stroke engine, the short circuiting process does not happen. Short circuiting happens when fresh intake charge is expelled through the exhaust port, which results in a significant source of unburned hydrocarbons. In a four stroke engine, the pressure inside the intake manifold is less than atmospheric (under *WOT* conditions, the pressure is approximately atmospheric). Since the pressure inside the engine cylinder is greater than atmospheric, when the intake valve is opened, a small amount of exhaust gases flow back into the intake port. This flow will reverse when the piston starts moving downward again, creating lower pressures within the cylinder.

This clear definition of cylinder events leads to higher combustion temperatures than two stroke engines, (due to the lack of intake dilution) and correspondingly higher NO_x emissions. In addition, the fuel consumption is approximately one third that of a two stroke engine and *HC* output is a factor of ten less. These significant differences lead

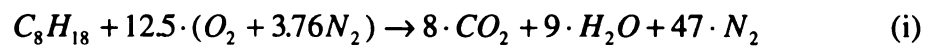
to an engine that is more fuel efficient and one that produces less *HC* emissions. Conversely, the four stroke engine is one that is more expensive to produce due to the increased parts list involved (camshaft and related valve gear).

1.3 Emission Characteristics of Small O.H.V. Four Stroke Engines

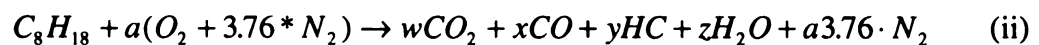
There are two main factors that influence emission output from small four stroke engines, relative to a stoichiometric mixture: 1) the operating air / fuel ratio and 2) the high relative combustion temperatures.

1.3.1 Emissions from rich air / fuel ratios

Small engines require air / fuel ratios that are slightly richer than stoichiometric, typically around 12:1 to 13:1. The abundance of fuel present within the mixture has three effects: 1) it increases *HC* output; 2) it increases *CO* output; and 3) it lowers the relative cylinder combustion temperature. In ideal combustion, all the fuel and oxygen is converted into *CO₂* and *H₂O*, according to equation (i):



In fuel rich combustion, there is relatively less oxygen, so fuel ends up being burned as *CO₂*, *CO* and unburned *HC*, according to equation (ii):



This equation by no means is a complete model of incomplete combustion. It is intended to show some of the possible combustion products when fuel rich combustion occurs.

The HC 's present in the equation are illustrative of all HC 's that result from excess fuel. Any excess products, other than CO_2 , H_2O and N_2 will result in a decrease in combustion temperature. The rich air / fuel mixtures inducted into these engines causes an increase in CO , HC and a decrease in combustion temperature.

1.3.2 Emissions from high temperature combustion

The inherent nature of four stroke engines is to have higher combustion temperatures than their two stroke counterparts. This is primarily due to the lack of short circuiting during the intake process. Since there is less exhaust gas present within the cylinder, the result is higher combustion temperatures and a corresponding increase in the formation of NO_x . Primarily this (high NO_x) is the main drawback of the four stroke engine, besides the increased initial cost. NO_x formation can be controlled with conventional emission control methods, such as Exhaust Gas Recirculation (EGR), and is found on automotive production four stroke engines today.

1.4 Literature Review

Many papers have been written on the subject of small engine emissions. However most four stroke engines are larger in displacement and of older design than the one tested in this study. In the early seventies, several papers were written on the subject of small engine emissions. During the early years of emission regulation (1972), small engines were considered only to contribute a small part of the total CO , HC and NO_x production.

Eccleston, and Hurn, [6] first analyzed exhaust emissions from small utility internal combustion engines, noting how the exhaust hydrocarbon composition differed

between two stroke and four stroke engines. More specifically the hydrocarbon composition within the exhaust of the two stroke engine closely mirrored that of the fuel. This was not the case for the four stroke, where the fuel was broken down into more basic carbon elements (see figure 1). This is a direct result of the short-circuiting event that happens during the scavenging process, where part of the intake charge escapes through the exhaust port.

Donohue, Hardwick, Newhall, Sanvordenker and Woelffer, [4] discuss the relevance of the emissions from these engines, estimating hydrocarbon emission output from these sources to be less than 1% of the total annual hydrocarbon output from all sources (see figure 2). Note: The scaling of the x axis, the output from the small engines, is an order of magnitude less. In addition they estimate of the total U.S. carbon monoxide output, totaling 100,000,000 tons/year, small engines contribute approximately 1,160,000 tons/year or approximately 1%. It is important to keep in mind that this data was formulated in 1968; current automotive production of emission products has been greatly reduced.

Hare, Springer, Oliver and Houtman, [9] estimated that emission production from small utility engines constituted only a small portion of the total pollution from all sources. They further estimated (as percentages of 1970 national totals from all sources) small engines account for 0.4% of *HC*'s, 0.8% of *CO* and 0.006% of *NO_x*. It was noted they rank second to highway vehicles in terms of the current number of engines in use. With very vigorous sales numbers each year, future weighting of emission output from these engines was likely to become more pronounced.

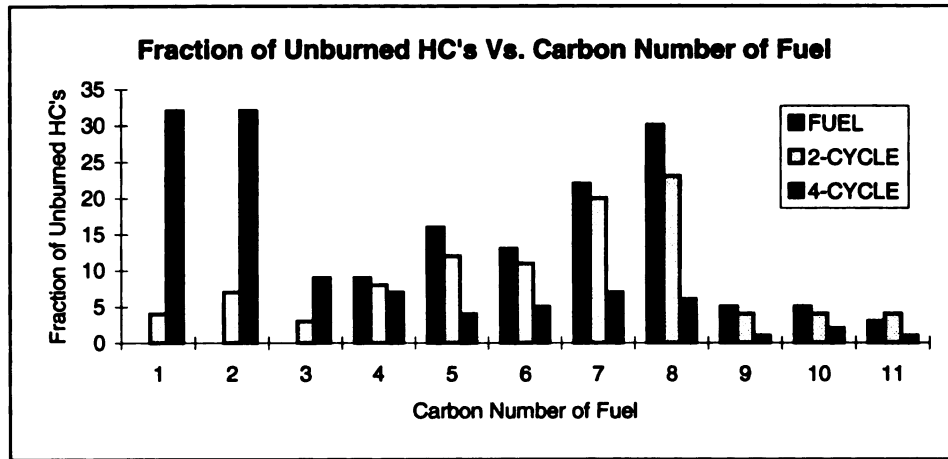


Figure 1: Composition of Exhaust and Fuel as a function of carbon number [6]

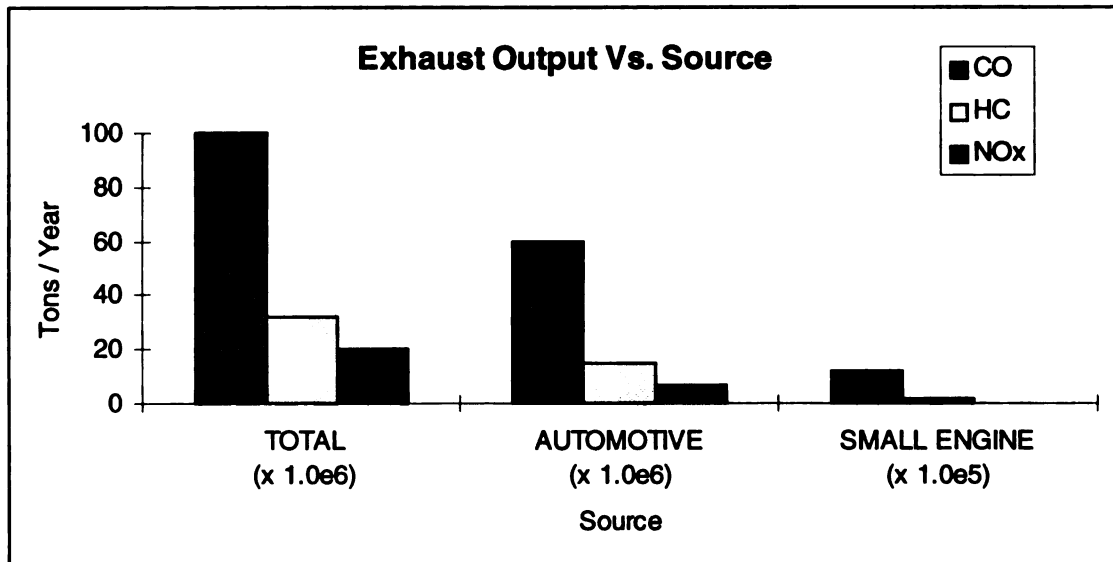


Figure 2: Exhaust Emission Sources [4]

In addition to previously being considered only a minor contributor in the global emission production, these engines produce very high amounts of HC , NO_x and CO for the power generated. Several papers have been written on the subject of reducing the output from these useful sources. White, Carroll, Hare and Lourenco [10] found that several traditional methods are effective in reducing emissions output from these engines. For example, leaner carburetor settings will reduce the CO output from these engines.

Conversely, leaner intake charges typically increase combustion temperatures and therefore the NO_x output, which is also a regulated emission species. In addition the leaner mixture increased cylinder head temperature and therefore may decrease engine life.

These results were confirmed by Sun, Assanis, and Brereton [12], who stated that traditional emission control approaches already in use in automobiles, work quite effectively. Some examples are catalytic converters, leaner mixture ratios and oxygenated fuels. Perhaps the biggest factor is the rich mixture ratios required by these small engines. The rich mixture ratios enhance engine life, promote engine cooling and extend engine power of small air-cooled engines. The disadvantage of this is high HC and CO emissions, increased cylinder temperatures, a reduction in engine life and the thermal destruction of any catalytic converter so attached.

Mooney, Shinn Hwang, Daby and Winberg [5] also reconfirmed the above conclusions. Specifically the reduction in mixture requirements were given the utmost attention. They speculate that meeting CARB Tier 1 and EPA Phase 1 emission regulatory levels might be accomplished with engine modifications only. CARB Tier 2 will probably require the application of catalytic converter technology to these engines. In order for the successful application of converter technology several areas of “lean burn” utility engines need to be addressed. For example: making these engines run leaner; catalyst durability and thermal stability; improving utility engine oil consumption; cooling air management / heat shielding and high temperature mounting systems.

Current California exhaust emission standards are quite stringent, compared to previous allowable pollution levels. Table 3 shows some of the allowed emission levels and compares them to current automotive standards. It should be noted that a typical

chain saw (tuned) emits 600 times the allowable CO and 250 times the allowable $HC + NO_x$ of a typical automobile on a brake specific basis. It is apparent that the practice of operating these engines at richer mixtures must be addressed before the reduction of exhaust components can be achieved.

Table 3: California Current Emission standards

| California Exhaust Emissions Standards for Off-Road Engines | | |
|---|--------------|--------------------|
| | CO(gr/kW-hr) | HC + NOx(gr/kW-hr) |
| California Regulation (1994) | 400 | 16 |
| California Regulation (1999) | 133 | 4 |
| Honda GXV120 (4 Hp), OHV 4-stroke | 640 | 25 |
| Lawnboy D410 (2Hp), 2-stroke (tuned) | 600 | 250 |
| Lawnboy D410 (2 Hp), 2-stroke (untuned) | 1500 | 800 |
| Homelite Series 200 Chainsaw (1 Hp), 2-stroke | 580 | 200 |
| Typical Automobile (light duty; 5 yrs/50,000 miles) | < 1 | < 0.1 |

1.5 Objectives

In general, there has been little work done in the area of ambient conditions and the effects on small engine emissions. Only a small amount of empirical work has been done in the area of automobile four stroke engines, but it is of little relevance to small engines. It would be of great benefit to understand the relationship between ambient conditions and engine emissions, in order to propose a standardized set of emission testing procedures. The general objectives of this thesis are:

- 1) To measure emission output as functions of ambient (pressure, temperature and humidity) conditions.

- 2) To explore the degree to which theoretical approaches can be used to reliably predict four stroke small engine emissions' dependence on ambient conditions.
- 3) To explain why changes in ambient conditions produce changes in measured emissions and engine power output.

2. EXPERIMENTAL METHODS

2.1 The Test Engine

The engine used throughout the testing procedure was the Ryobi Pro4Mor Over Head Valve (OHV) engine. This is the first portable hand-held gasoline engine capable of meeting all proposed U.S. exhaust emission standards for lawn and garden equipment, including 1999 CARB standards. A table summarizing the engine characteristics is given below (see table 4).

Table 4: The Test Engine

| | |
|-----------------|--------------------------|
| BORE | 3.2 cm |
| STROKE | 3.26 cm |
| DISPLACEMENT | 26.2 cc |
| RATED kW | .75 @ 7000 RPM |
| CONFIGURATION | OHV - PUSH ROD |
| ROCKER ARM TYPE | STAMPED STEEL, BALL TYPE |
| MASS | 3.6 kg |

2.2 Climate Control

The Ryobi Pro4Mor OHV engine was run over a range of ambient conditions. For example the temperature was varied from 9.53 °C to 29.03 °C (holding the humidity constant) and the humidity was varied from 0.01487 kg H_2O /kg AIR to 0.00578 kg H_2O /kg AIR (holding the temperature constant). Two types of tests were performed: one at constant ambient temperature while varying humidity; and the other at constant

ambient humidity while varying temperature. As a result, it was possible to measure the emission output as a function of room temperature, room relative humidity or both.

2.3 Experimental Apparatus

In order to measure the emission output from small engines, several pieces of equipment are required. They are summarized in table 5 below:

Table 5: Equipment Used

| FUNCTION | APPARATUS |
|------------------------------------|--|
| Engine Controls | Micro-Dyn Dynamometer Model 15 |
| Exhaust-gas collection | Dilution tunnel with 100 scfm critical-flow nozzle |
| Fuel flow measurement | Micro Motion Fuel Meter DS0006S100 |
| CO and CO ₂ measurement | Horiba Infrared Analyzer AIA-23 |
| NO _x measurement | Horiba Chemiluminescent Analyzer CLA-22A |
| HC measurement | Horiba Flame Ionization Analyzer FIA-23A |
| Temperature Controls | Honeywell Industrial Temperature Controls T-775-A |
| Humidity Controls | Honeywell Industrial Humidity Controls T-775-E |
| Data Collection | IBM 486 PC With 3 Digital to Analog Boards |

A brief description of each piece of equipment follows. The engine was run on a hydraulic dynamometer which allowed it to run at a programmed constant speed (RPM), while measuring the torque output produced by the engine. Fuel was supplied to the engine by a custom-built fuel cart, which measured the mass flow rate of fuel consumed by the engine. Fuel was supplied to the engine at constant pressure. The intake of the dilution tunnel was positioned so that all the exhaust products and large quantities of room air were drawn into the tunnel, without placing additional suction on the muffler exit. This diluted mixture of exhaust gas was drawn through a critical flow nozzle by a ring compressor, which regulates the total flow rate of ambient air and exhaust gases. A

sample of this diluted gas was fed to the emission analyzers while the remainder was expelled from the test room. The analyzers measured the diluted gas for concentrations of HC , NO_x , CO_2 and CO . Figure 3 gives a general overview of the test cell. For more complete details on equipment used, refer to Appendix A.

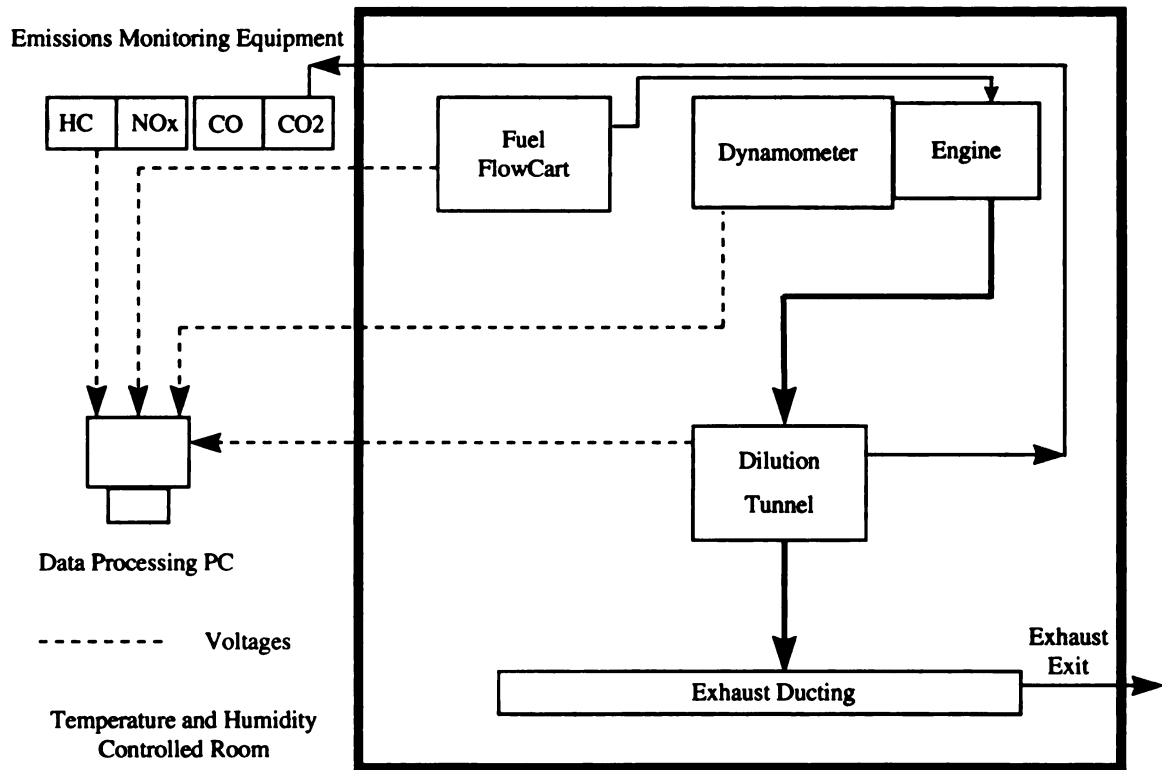


Figure 3: Overview of Test Cell

2.4 Experimental Procedure

For each test conducted (either humidity or temperature ramp) the room was set to the desired value (temperature or humidity), and allowed to stabilize overnight. After the desired value had been attained, the necessary equipment was switched on and calibrated.

No two tests were performed on the same day and the engine was not operated for more than 1.5 hours continuously.

For each test, the engine was operated at Wide Open Throttle (*WOT*) or approximately 7000 rpm. During this time the engine and emission analyzers were allowed to stabilize before any measurements were taken. Once the equipment had reached steady state, the temperature or humidity could be altered.

2.4.1 Measured Quantities

Many quantities had to be measured to calculate the emission output from the engine. A brief rundown of the important items are listed below.

The concentrations of all emission species involved were measured. They include: *HC*, *NO_x*, *CO₂* and *CO*. Additional quantities that are measured include: the speed of the engine, torque output, the atmospheric and differential pressure. The differential pressure is the stagnation pressure ahead of the critical flow nozzle. The temperatures include: the temperatures of the nozzle (temperature of air just ahead of the critical flow nozzle), cylinder head, exhaust, fuel, room air (at engine air inlet) and engine oil. Relative humidity and fuel flow rates were also quantified. See Appendix E for a sample listing.

2.4.2 Calibration

The dynamometer, emission bench, and fuel cart were all calibrated initially and checked periodically. The torque calibration on the dynamometer was performed by hanging a 1 kg mass (2.2 lb.) a distance of 45.72 cm (18 inches) from the centerline. This

known torque generated a voltage and was used along with the zero point, to generate a linear relationship between torque and voltage.

Calibration of the fuel flow meter was performed by Micro Motion. It was checked by flowing fuel through the meter for a known time. This volume of fuel collected (in units of cm^3/sec) was converted to gr/hr and compared to the meter reading. This verified the Micro-Motion calibration. Other outputs from the fuel flow cart include the ambient temperature and humidity levels. They were calibrated in a similar manner to the torque meter. For the temperature output, the room was set to a reference temperature, verified with four thermometers and compared to the voltage output. Likewise for the humidity, with the exception that only two meters were used to double check the room humidity and then compared to the voltage output. This allowed algebraic linear relationships between temperature, humidity and voltage, to be found that could be used for subsequent data reduction.

Calibration of the emission analyzers was performed in a similar manner. The meters were calibrated daily or before each run using two gases of known concentrations. A “zero” gas (pure N_2) was supplied to the analyzer to set the zero point and the “span” gas supplied to the analyzer set the full scale reading. The meters were all tested for linearity, using a gas divider and the appropriate span gas. A gas divider controls (or decreases) the proportions of span and zero gas fed to the meter. This allows one to record analyzer voltage outputs, for a range of known concentrations and plot the results to check for linearity. Three of the four meters varied linearly with the span gas (CO_2 , HC and NO_x) while the fourth (CO) was found to be well approximated by a second order polynomial. The algebraic equations inferred from these calibrations were used to convert analyzer output voltages to concentrations.

2.4.3 Temperature Variation

In order to perform the temperature transient, the room was set to a specified cold temperature (0 °C) and allowed to stabilize overnight. With all the equipment running the coolers were turned off, the heater was switched on, and the room was allowed to warm up. As the room warmed up, the emission characteristics of the engine were measured. The ambient humidity level increased slightly as the room temperature increased.

2.4.4 Humidity Variation

Likewise for the humidity variation. In order to perform the humidity ramp, the room was set to a specified humidity level ($0.015 \text{ kgH}_2\text{O/kgAIR}$) and allowed to stabilize overnight. With all the equipment running, the humidifier was turned off, which allowed the ambient moisture levels to drop. As the moisture level dropped, the emission characteristics of the engine were measured. As with the temperature transient, the ambient temperature level increased slightly as the room humidity decreased.

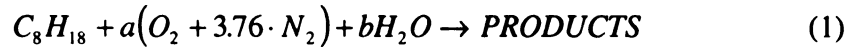
The room humidity was controlled by a steam generator and a Honeywell model T775-E remote humidity sensor. It was easier to de-humidify the room than to humidify, so for each test the humidity was set to a high initial value and allowed to stabilize overnight. Then, with all the equipment running, the steam generator was turned off and the humidity level was allowed to drop. This gave the desired rate of decrease in ambient humidity and allowed engine emissions to be measured as a function of specific humidity.

3. RESULTS

The results chapter is divided into three parts: a theoretical section concerned with thermodynamic analyses of gasoline combustion; a theoretical results section and an experimental section in which measurements are reported and discussed.

3.1 Theoretical Equations

In order to do combustion analysis, one must first specify the properties of the reactants. For example, during the combustion of moist air + fuel, the Air Fuel Ratio (*AFR*) and specific humidity (ω) determine the number of moles of air (a) and water vapor (b) in the reactants. According to equation (1), fuel reacts with a moles of air and b moles of water vapor to form combustion products. The following sections (3.1.1, 3.1.2 and 3.1.3) describe the thermodynamic modeling used for carburation, compression and combustion, respectively.



3.1.1 Carburation

Assuming, for convenience, that 1 *kmol* of fuel is present, the moles of air and water vapor are completely determined by the specific humidity and the *AFR* according to relations (2) and (3) below.

$$\omega = \frac{m_{H_2O}}{m_{AIR}} = \frac{n_{H_2O} M_{H_2O}}{n_{AIR} M_{AIR}} = \frac{18b}{29a} \text{ or } b = \frac{29a\omega}{18} \quad (2)$$

$$AFR = \frac{m_{AIR}}{m_{FUEL}} = \frac{a(32 + 3.76 \cdot 28)}{1 \cdot 114} = 1.2042 \cdot a \quad (3)$$

Thus, with the specific humidity and AFR set, the LHS of the combustion equation is fully determined. In the following discussion, it is shown how, when the carburetor throat is the limiting area, carburetors regulate the quantity $(\dot{m}/\sqrt{\rho})$ or $(\dot{V}\sqrt{\rho})$.

Figure 4 gives the reference points used in the following equations.

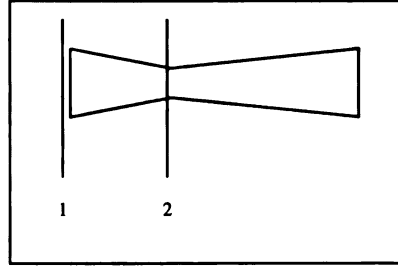


Figure 4: Cross section of Carburetor throat

Treating the flow from intake (position 1) to throat (position 2) as steady, friction less and incompressible (due to the compressibility effects being negligible, see appendix C for notes on compressibility), the Bernoulli equation states that,

$$\frac{P_1}{\rho} + \frac{V_1^2}{2} = \frac{P_2}{\rho} + \frac{V_2^2}{2} \quad (4)$$

$$V_2 = \sqrt{\frac{\frac{2}{\rho}(P_1 - P_2)}{\left(1 - \frac{V_1^2}{V_2^2}\right)}}$$

Since $V_1^2/V_2^2 \approx 0$ and $P_1 - P_2$ is almost constant for a carburetor at a given throttle setting. Then $\sqrt{\rho}V_2 = \text{CONSTANT}$, or for a fixed throat area ($\dot{V} = VA$),

$$\dot{V}\sqrt{\rho} = \text{CONSTANT}. \quad (5)$$

Starting with, the ideal gas equation,

$$PV = n\bar{R}T,$$

under steady flow conditions differentiating both sides with respect to time leads to,

$$P\dot{V}_{MIX} = \dot{n}_{MIX} \bar{R}_{MIX} T \text{ or } \dot{V}_{MIX} = \dot{n}_{MIX} \bar{R}_{MIX} \left(\frac{T}{P} \right)$$

where \dot{V} is the volume flow rate and \dot{n} is the molal flow rate of air and water vapor. Substituting the above relation into (5) and setting $\dot{n}_{MIX} = (\dot{n}_{AIR} + \dot{n}_{H_2O})$ yields the following relation (with \bar{R} absorbed in the *CONSTANT*),

$$\left(\dot{n}_{AIR} + \dot{n}_{H_2O} \right) \left(\frac{T}{P} \right) \sqrt{\rho_{MIX}} = \text{CONSTANT}, \quad (6)$$

with ρ_{MIX} as the density of air and water vapor. Furthermore, since P was essentially constant throughout each experiment run in this study, equation (6) reduces to,

$$\left(\dot{n}_{AIR} + \dot{n}_{H_2O} \right) T \sqrt{\rho_{MIX}} = \text{CONSTANT} \quad (7)$$

Next, letting $\dot{n}_{AIR} + \dot{n}_{H_2O}$ equal $\dot{a} + \dot{b}$ (as in equation (1)),

$$\left(\dot{a} + \dot{b}\right) T \sqrt{\rho_{MIX}} = \text{CONSTANT} . \quad (8)$$

Substitution for the density of the mixture in terms of convenient parameters, requires additional derivation. Starting with the density of the mixture, ρ_{MIX} , which equals:

$$\rho_{MIX} = \frac{m_{AIR} + m_{H_2O}}{V} = \frac{\rho_{AIR} V_{AIR} + \rho_{H_2O} V_{H_2O}}{V} = \frac{\rho_{AIR} n_{AIR}}{n_{TOTAL}} + \frac{\rho_{H_2O} n_{H_2O}}{n_{TOTAL}}$$

we can write,

$$\rho_{MIX} = \frac{\rho_{AIR} n_{AIR}}{n_{TOTAL}} + \frac{\rho_{H_2O} n_{H_2O}}{n_{TOTAL}}$$

or dividing by the density of air,

$$\frac{\rho_{MIX}}{\rho_{AIR}} = \frac{n_{AIR}}{n_{TOTAL}} + \frac{\rho_{H_2O}}{\rho_{AIR}} \frac{n_{H_2O}}{n_{TOTAL}} . \quad (9)$$

Next, from the ideal gas law,

$$PV = \frac{m}{M} \overline{RT} \Rightarrow \frac{PM}{\overline{RT}} = \frac{m}{V} \Rightarrow \frac{PM}{\overline{RT}} = \rho \quad (i)$$

which leads to,

$$\frac{\rho_{H_2O}}{\rho_{AIR}} = \frac{\frac{PM_{H_2O}}{RT}}{\frac{PM_{AIR}}{RT}} = \frac{M_{H_2O}}{M_{AIR}} = \frac{18}{29}. \quad (ii)$$

Substituting the above relation (ii) into equation (8) and noting that $n_x = \frac{m_x}{M_x}$,

$$\frac{\rho_{MIX}}{\rho_{AIR}} = \frac{\frac{m_{AIR}}{M_{AIR}}}{\underbrace{\left(\frac{m_{AIR}}{M_{AIR}} + \frac{m_{H_2O}}{M_{H_2O}} \right)}_{n_{TOTAL}}} + \frac{18}{29} \frac{\frac{m_{H_2O}}{M_{H_2O}}}{\underbrace{\left(\frac{m_{AIR}}{M_{AIR}} + \frac{m_{H_2O}}{M_{H_2O}} \right)}_{n_{TOTAL}}},$$

dividing the numerator and denominator by the mass of air, yields

$$\frac{\rho_{MIX}}{\rho_{AIR}} = \frac{\frac{m_{AIR}}{m_{AIR} M_{AIR}}}{\left(\frac{m_{AIR}}{M_{AIR} m_{AIR}} + \frac{m_{H_2O}}{M_{H_2O} m_{AIR}} \right)} + \frac{18}{29} \frac{\frac{m_{H_2O}}{m_{AIR} M_{H_2O}}}{\left(\frac{m_{AIR}}{M_{AIR} m_{AIR}} + \frac{m_{H_2O}}{M_{H_2O} m_{AIR}} \right)}$$

or,

$$\frac{\rho_{MIX}}{\rho_{AIR}} = \frac{1}{\underbrace{M_{AIR}}_{29} \left(\frac{1}{M_{AIR}} + \frac{\omega}{M_{H_2O}} \right)} + \frac{18}{29} \frac{\omega}{\underbrace{M_{H_2O}}_{18} \left(\frac{1}{M_{AIR}} + \frac{\omega}{M_{H_2O}} \right)} = \frac{1 + \omega}{1 + \frac{29}{18} \omega}. \quad (10)$$

From the definition of specific humidity [23],

$$\omega = \frac{m_{H_2O}}{m_{AIR}} = \frac{18}{29} \frac{P_{H_2O}}{P_{AIR}}$$

$$P_{MIX} = P_{AIR} + P_{H_2O} = P_{AIR} \left(1 + \frac{29\omega}{18} \right)$$

$$\rho_{AIR} = \frac{P_{AIR}}{R_{AIR} T} = \frac{P_{MIX}}{\left(1 + \frac{29\omega}{18} \right) R_{AIR} T}$$

and for experiments conducted at constant P_{MIX} ,

$$\rho_{AIR} \propto \frac{1}{\left(1 + \frac{29\omega}{18} \right) T}.$$

Substituting for ρ_{MIX} and ρ_{AIR} , as indicated in (8) and above into (10),

$$\left(\dot{a} + \dot{b} \right) T \sqrt{\frac{(1+\omega)}{T \left(1 + \frac{29}{18} \omega \right)^2}} = CONSTANT.$$

Next, substituting for b in terms of a from (2),

$$a \left(1 + \frac{29}{18} \omega \right) T \sqrt{\frac{(1+\omega)}{T \left(1 + \frac{29}{18} \omega \right)^2}} = CONSTANT$$

or,

$$a = \frac{CONSTANT}{\sqrt{(1+\omega)T}}. \quad (11)$$

We define the molal flowrate of air at $T = T_{REF}$, $\omega = 0$ as the design air flow rate, a_d . In which case $a_d \sqrt{T_{REF}} = \text{CONSTANT}$ or,

$$a = a_d \sqrt{\frac{T_{REF}}{(1 + \omega)T}} \quad (12)$$

Since the fuel flow rate is determined by the vacuum at the carburetor throat, which is essentially fixed at a given throttle opening, then from (3),

$$\frac{AFR_d}{a_d} = 1.2042 = \frac{AFR_a}{a_a}$$

or,

$$a_d = \frac{AFR_d}{1.2042}. \quad (13)$$

which leads to,

$$a = \frac{\frac{AFR_d}{1.2042}}{\sqrt{(1 + \omega) \left(\frac{T}{T_{REF}} \right)}} \text{ and } b = \frac{29a\omega}{18}$$

and,

$$AFR_a = \frac{AFR_d}{\sqrt{(1 + \omega) \left(\frac{T}{T_{REF}} \right)}} \quad (14)$$

Equation 14 states that for any given AFR_d (i.e. for a given fixed-jet carburetor in which the throat area is the limiting area to air flow), the actual AFR (AFR_a) is a function of temperature and specific humidity. The AFR_a is the actual AFR in a constant pressure test.

If there is an increase in specific humidity, the molal flowrate of air (a) will decrease therefore the AFR_a will also decrease (become richer). Likewise, if the temperature becomes greater than the reference temperature (T_{REF}), the AFR_a will also decrease (become richer).

Since the number of moles of a (air), b (H_2O) are determined using specific humidity (ω), T_{REF} , T and AFR_d , the molal flow rate of a and b is a function of AFR_d , ω and temperature. This allows the final temperature and pressure, at the end of compression to be calculated, for various operating (ω , T_{REF} , T , AFR_d) conditions.

3.1.2 Compression

Modeling the compression process can be accomplished in many ways: one can choose to treat the process as ideal (isentropic, constant C_p); one can have isentropic compression with temperature dependent properties, or one can have the actual case, with specified heat transfer and temperature dependent properties. It was decided to model compression as isentropic with temperature dependent properties, due to the difficulty in either determining the entropy produced in such a process, or equivalently, prescribing the heat transfer.

From the first law,

$$dQ - dW = dE \quad (15)$$

with

$$dE = dU .$$

If the process is ideal (i.e. reversible),

$$\begin{aligned} dW &= PdV \\ dQ &= TdS \end{aligned} \quad (16)$$

Substituting the above relations into (15) yields, the Gibbs relation:

$$TdS - PdV = dU \text{ or } dS - \frac{PdV}{T} = \frac{dU}{T} \quad (17)$$

Using the ideal gas law ($P/T = R/v$), constant entropy ($dS = 0$) and the definition for C_v ($C_v = dU/dT$) one obtains:

$$-\frac{R}{v}dv = \frac{C_v}{T}dT \quad (18)$$

Upon integrating both sides and rearranging, the following will result:

$$-R \ln \left(\frac{v_2}{v_1} \right) = \int_1^2 \frac{C_v}{T} dT \quad (19)$$

where C_v is a $f(T)$ and is mass weighted for each species in the reactants, according to:

$$C_{v,mix} = \frac{\sum_{i=1}^n m_i (c_v)_i}{\sum_{i=1}^n m_i} \quad (20)$$

Once the temperature dependence of the various specific heats are known, they can be integrated from a reference temperature to any final temperature, T_2 , and thus the Right Hand Side (RHS) of the above equation (19) is a function of T_2 . Since the volume ratio is the compression ratio, which is constant, the *LHS* is also known. This sets up an iteration process, where the final temperature is guessed and compared to the value on the *LHS*. The process is repeated until the *LHS* matches the *RHS*, at that point the guessed temperature is the temperature which is sought and the process repeats for different initial temperatures, humidity ratios and *AFR*'s. The compressed charge temperature T_2 and pressure P_2 are the conditions at which combustion calculations begin, according to figure 5 below.

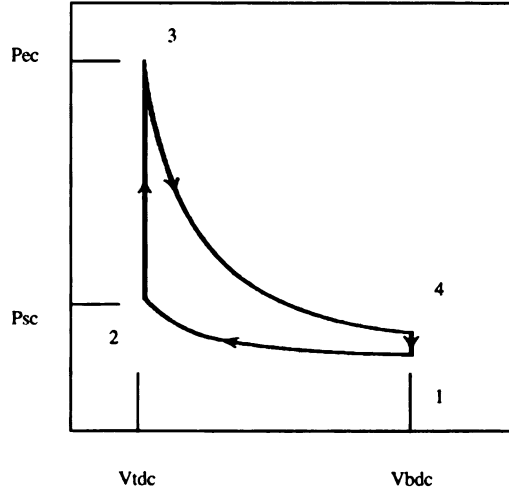


Figure 5: Pressure - Volume Diagram

3.1.3 Combustion

Several computer codes were used in generating the theoretical data. Along with the several FORTRAN codes utilized, a program called STANJAN [14] was used to analyze, and predict, the resulting combustion products, properties and composition. STANJAN is a set of FORTRAN computer programs developed at Stanford University for the analysis of *chemical equilibrium* problems arising in combustion and other applications. The program has the ability to treat mixture of ideal gases, condensed phases and separated incompressible solids or liquids, using the method of element potentials and the JANNAF thermo-chemical database. A driver program was written to predict the end of compression temperatures and pressures, assuming isentropic compression with temperature dependent properties. This program varied the specific humidity and starting temperature to determine the final pressure and temperature of the reactants. It then called STANJAN to calculate the composition and equilibrium state of the products, assuming a constant volume, constant energy process. The condition for equilibrium was that the Gibbs function of the mixed products was minimized. In carrying out these calculations, it was necessary to specify the possible species which comprise the products of hydrocarbon combustion.

The assumed products are taken from Heywood [19], pp. 93, figure 3-10-c. This figure illustrates possible products at a combustion temperature of 2750 K, 30 atm for various equivalence ratios. The list of the possible products is: N_2 , H_2O , CO_2 , CO , H_2 , OH , NO , NO_2 , O_2 and H .

The theoretical CO/CO_2 ratio was calculated using chemical equilibrium equations, taken from Spindt [8] and Heywood [19]. A good correlation between temperature and data suggests the reaction is frozen at a temperature of 1700 K [8], [19].

This suggests a value for K_p of 3.388, where K_p is the equilibrium constant. See appendix D for a sample of equations used.

3.2 Theoretical Results

Using the assumptions and equations of the previous section, a series of carburation, compression and combustion calculations were carried out at different ambient conditions.

The effect of ambient temperature on AFR (at $\omega = 0.005$), as a function of design AFR is shown in figure 6. The design AFR (AFR_d) is the AFR that one obtains using specified carburetor parameters, i.e. for a specified throat diameter and jet size. The actual AFR (AFR_a) is the one delivered to the engine by the carburetor, after the effects of temperature and humidity have been factored in. One can see that as the room temperature increases, the AFR_a becomes richer. This is expected, as the air becomes slightly less dense, there is more fuel available and thus the AFR is altered to a more rich setting.

Figure 7 shows the peak combustion temperature vs. AFR_a , at a constant ω . This plot indicates that for a fixed AFR , the initial temperature shifts the peak temperature upwards. The temperature increases to a maximum around an AFR_a of 14:1 and then the combustion temperature starts to fall off, as expected. It is well known that best power is obtained at a slightly rich setting, stoichiometric being 14.7:1. The peak temperature at an AFR of ~14:1 would theoretically deliver the maximum temperature and thus the maximum power. The effect of humidity is to shift the entire curve down as water vapor is added to the mixture.

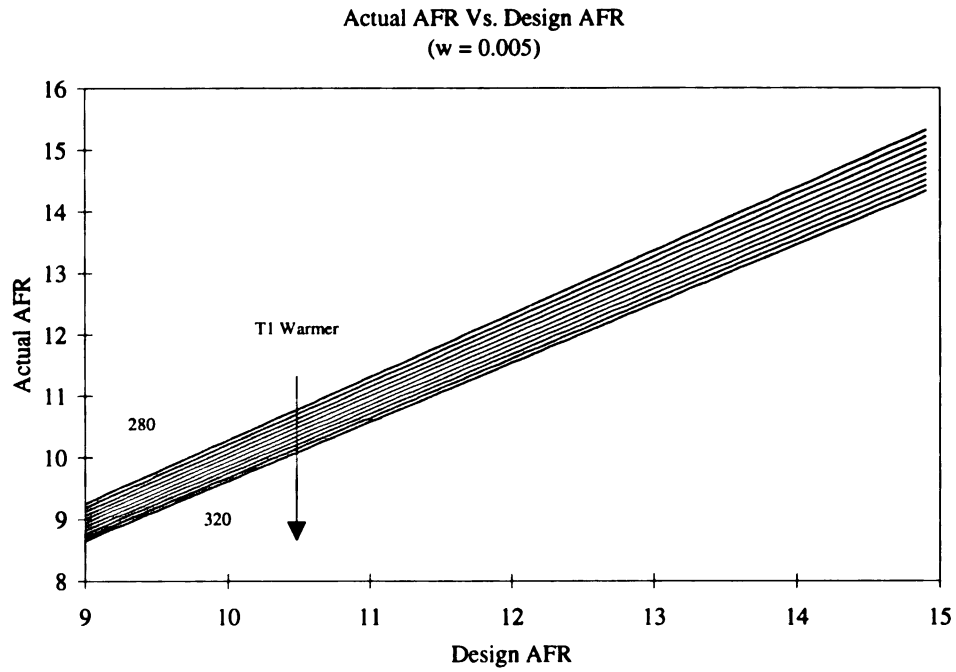
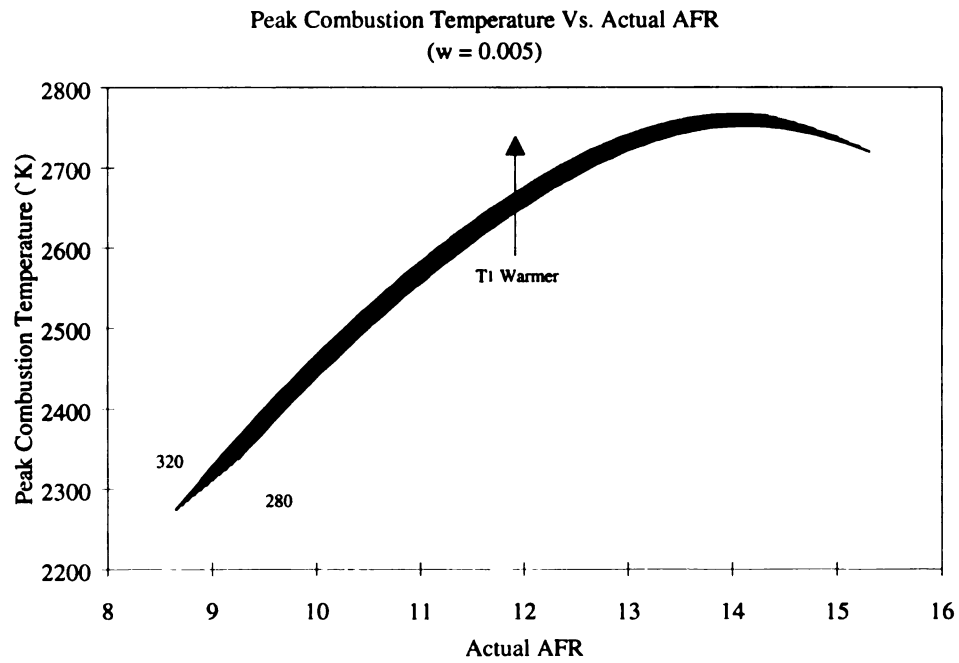
Figure 6: Actual *AFR* Vs. Design *AFR*Figure 7: Combustion Temperature Vs. Actual *AFR*

Figure 8 shows the combustion temperature as a function of the AFR_d . Again, the design AFR is the AFR that one obtains using specified carburetor parameters, i.e. for a specified throat diameter and jet size. It does not include correction factors for ambient temperature and humidity. This curve is generated using the same code, except the AFR is not modified for ambient conditions. On this plot, $T_1=280$ yields the highest temperature, while $T_1=320$ yields the lowest temperature. It is interesting to note how the curves transpose after an AFR_d 13:1. This is not the case when the peak temperature is plotted versus AFR_d , indicating that carbureted engines performance cannot be optimized without taking into account the local ambient conditions.

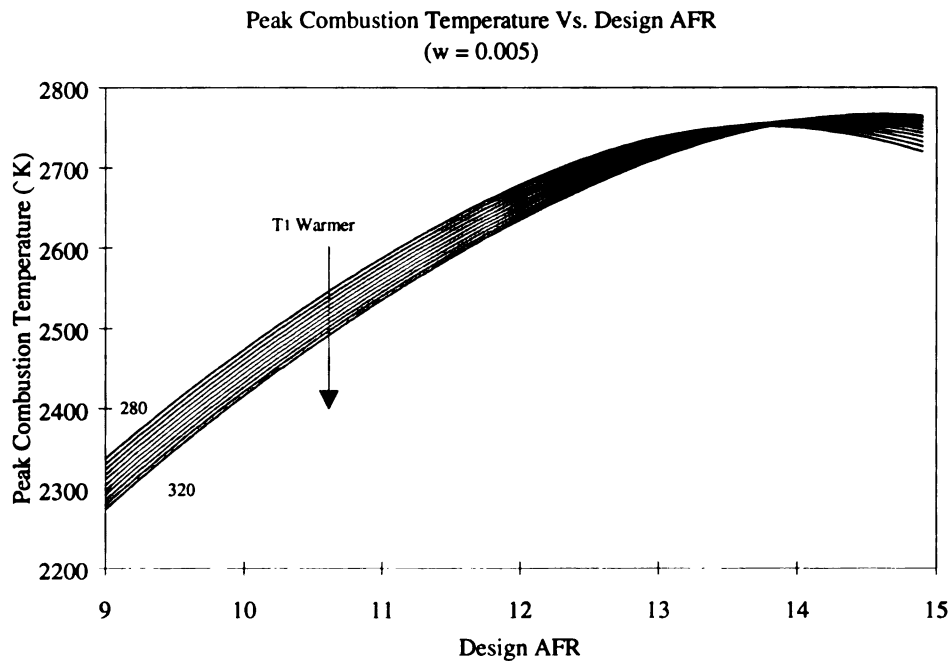


Figure 8: Combustion Temperature Vs. Design AFR

Figure 9 shows the effect of ambient humidity on AFR (at $T = T_{REF}$), as a function of AFR_d . Adding moisture to the ambient moisture levels did not effect the AFR_d as strongly as the temperature change did. The effect of increasing humidity has less of an effect on the AFR_d compared to increasing ambient temperature. The temperature change resulted in a 6.7% decrease in the theoretical AFR_d , a corresponding humidity change netted only a 0.78% drop in the theoretical AFR_d .

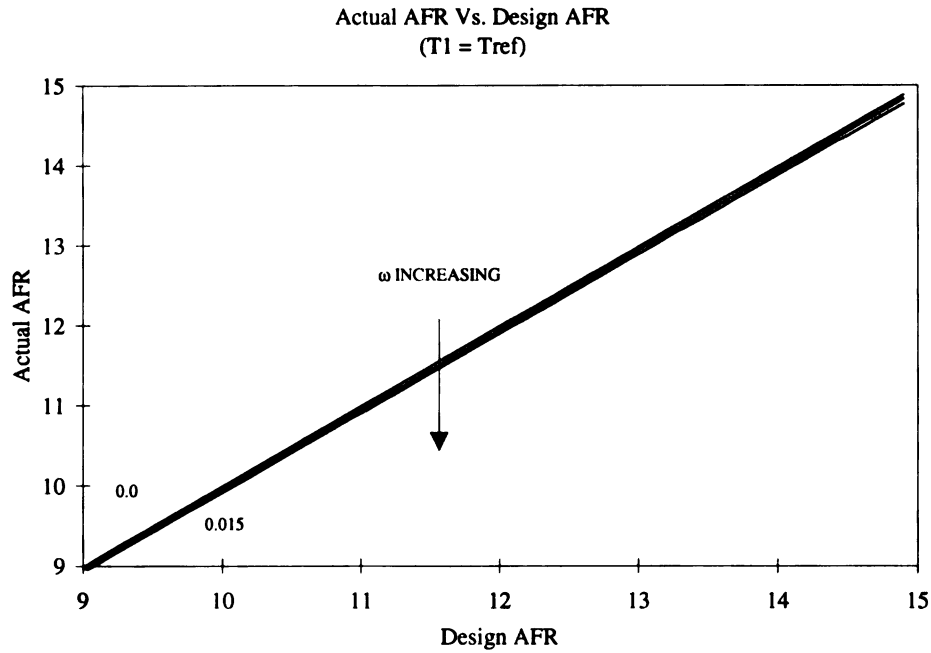
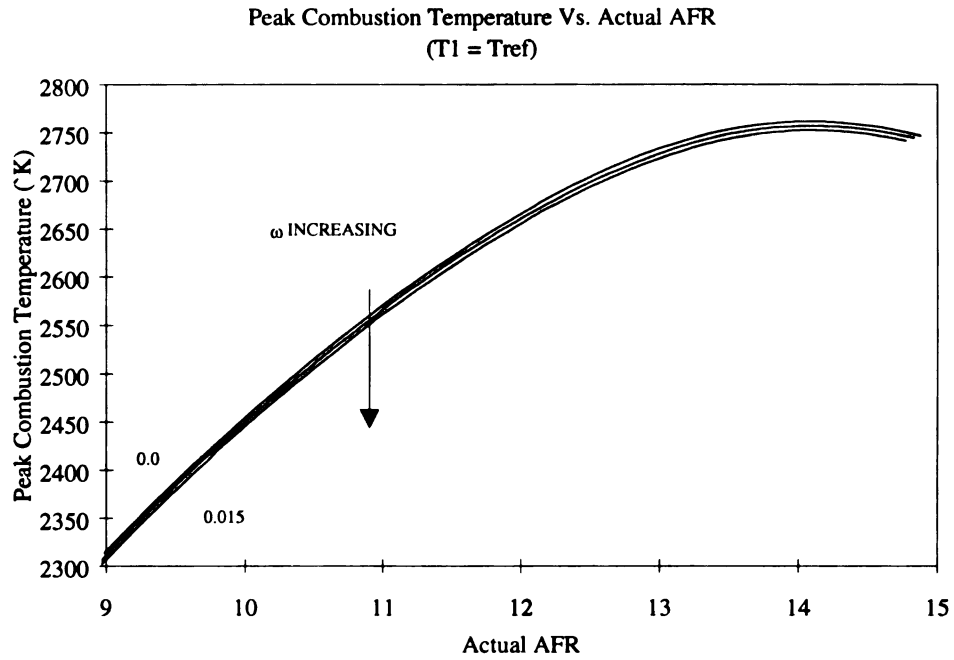
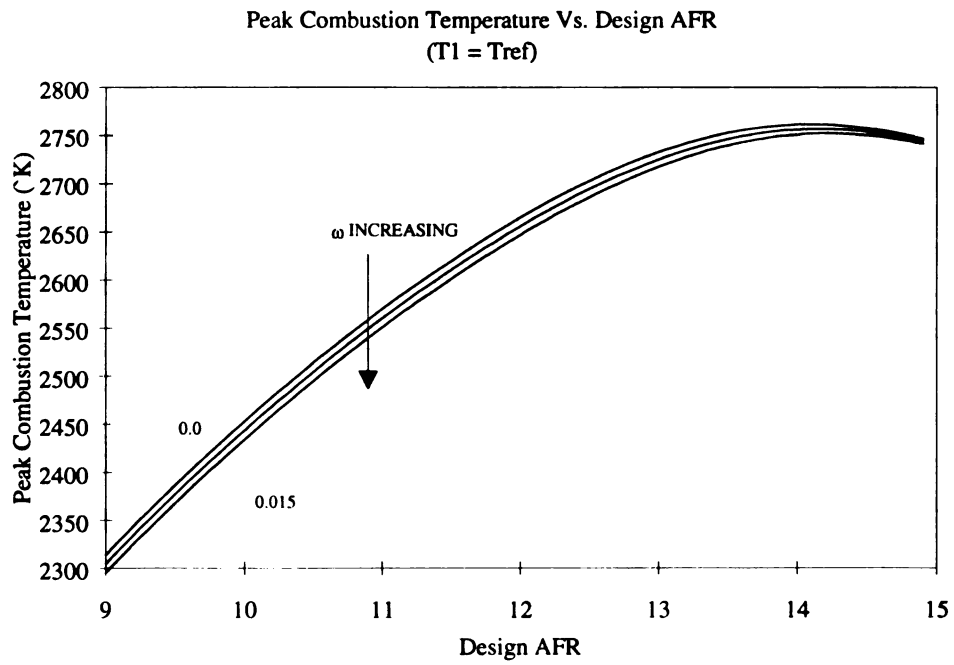


Figure 9: Actual AFR Vs. Design AFR

Figures 10 and 11 show the peak combustion temperature vs. AFR_d and AFR_a , respectively (at $T = T_{REF}$). The effect of adding moisture to the surroundings, shifts the peak combustion temperatures lower. This is due to the fact that the energy of the products is raised, so a lower temperature is required for chemical equilibrium at the same mixture energy.

Figure 10: Peak Combustion Temperature Vs. Actual *AFR*Figure 11: Peak Combustion Temperature Vs. Design *AFR*

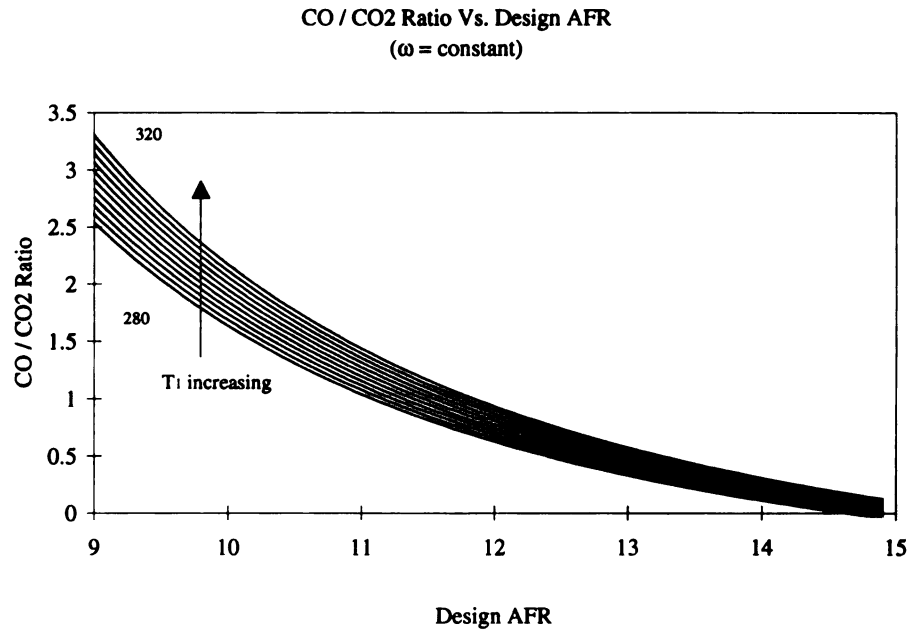
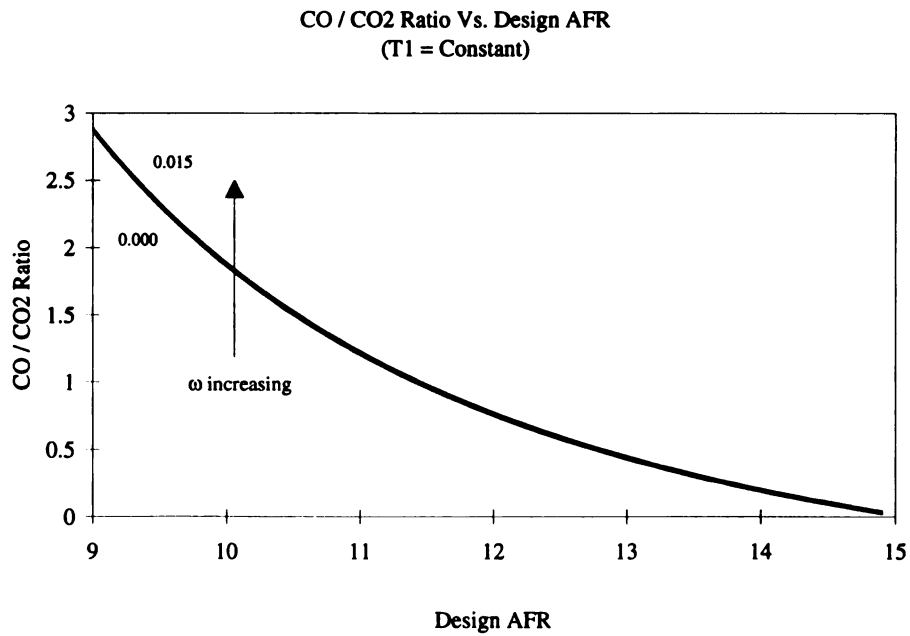
Figure 12: CO/CO₂ Ratio Vs. Design AFR (1)Figure 13: CO/CO₂ Ratio Vs. Design AFR (2)

Figure 12 and 13 show the theoretical CO/CO_2 ratio as functions of AFR_a . Figure 12 illustrates the effect of increasing ambient temperature at a constant humidity. As the temperature becomes warmer, the air becomes less dense, thus altering the AFR_a to a more rich setting. As the AFR_a becomes richer, more CO is produced and less CO_2 is formed (due to the lack of oxygen). Likewise figure 13 shows the effect of increasing ambient humidity, while holding ambient temperature levels constant. This figure shows the effect on AFR_a as humidity is increased. This enrichment causes more CO to be produced and less CO_2 to be made, thus increasing the CO/CO_2 ratio.

While the variation of CO/CO_2 with changing humidity is slight, the dependence on ambient temperature is significant, especially at rich AFR 's (figure 12).

3.3 Experimental Results

Three engine tests were performed: an idle test varying the surrounding temperature; a *WOT* test varying the humidity at constant temperature; and a *WOT* test varying the temperature at constant humidity.

The tests carried out at *WOT* are the most applicable to theoretical analysis and their results are described in detail below.

3.3.1 Humidity Variation

Figure 14 displays room temperature versus specific humidity. This shows that room temperature remains essentially constant throughout the entire test. The temperature varied a total of 1.4%.

Engine performance changed little with modest changes in the surrounding humidity. The humidity was varied from ~ 0.015 ($kgH_2O/kgAIR$) to $.006$ ($kgH_2O/kgAIR$) or -150%. Throughout this range, the torque output remained essentially constant, varied slightly from $.75$ N-m. Figure 15 shows torque vs. specific humidity. At the higher humidities, torque decreases slightly with increasing humidity; this is consistent with the dry air mass in the cylinder decreasing with increasing ω as predicted by (14).

Brake Specific Fuel Consumption (BSFC) is also an important engine operating parameter. It is given by the following equation:

$$BSFC = \frac{\text{fuel flow}(gr/hr)}{\text{power}(kW)} \quad (21)$$

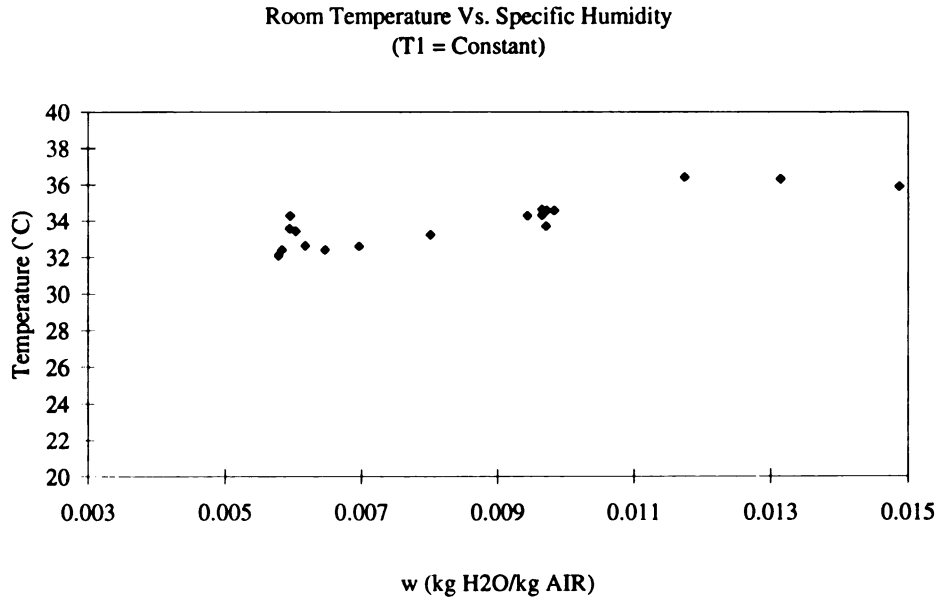


Figure 14: Room Temperature Vs. Specific Humidity

Figure 16 shows BSFC vs. specific humidity. It is shown to increase slightly over the range of the test. This is expected, as the moisture level is increased, the *AFR* will decrease slightly. This slight decrease in *AFR* (richer mixture) causes the air flow rate to rise, causing the engine torque to slightly increase.

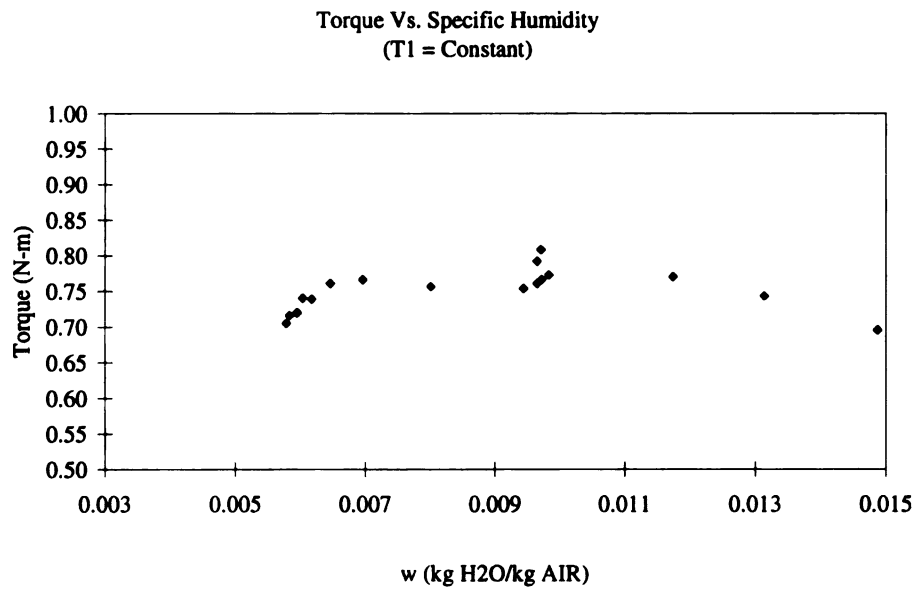


Figure 15: Engine Torque Vs. Specific Humidity

CO is plotted versus ambient humidity as in figure 17. *CO* increases slightly with increasing specific humidity, and this is expected. As the air becomes more humid, the *AFR* ratio will decrease, resulting in a richer mixture. As the mixture becomes richer, more *CO* is produced, due to the decreasing amount of oxygen, which is needed for stoichiometric combustion.

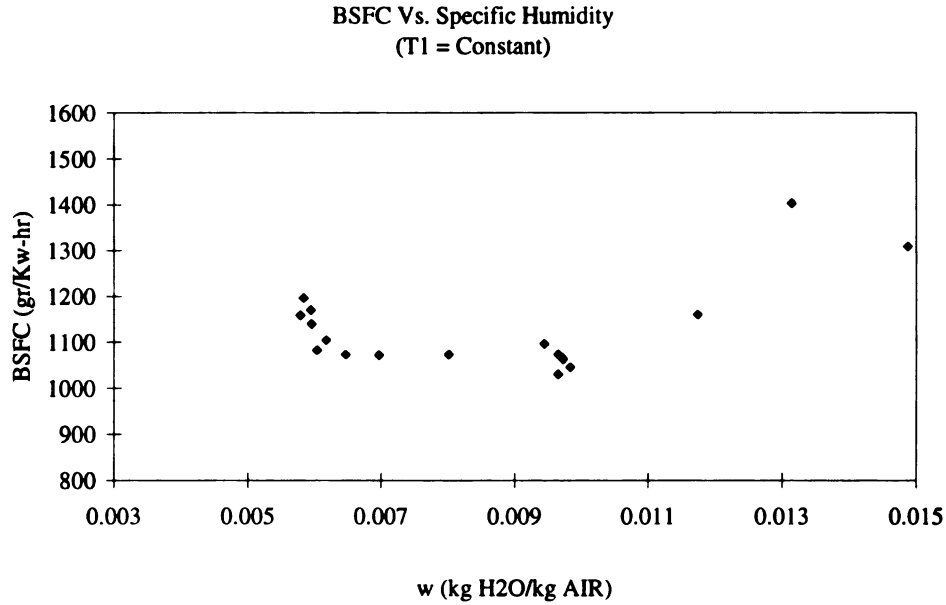


Figure 16: BSFC Vs. Specific Humidity

CO_2 is plotted against specific humidity in figure 18. As the specific humidity level increases the mixture *AFR* decreases (becomes richer), resulting in less oxygen available for combustion. With less oxygen, less CO_2 is produced. This is seen in the figure.

The trends for NO_x reveal a similar pattern to that observed for CO . Figure 19 illustrates how the NO_x level decreases as the humidity increases (*AFR* decreasing). As the *AFR* decreases, the combustion temperature drops. When the combustion temperature drops, the formation of NO_x is lowered significantly, due to the large temperature dependence.

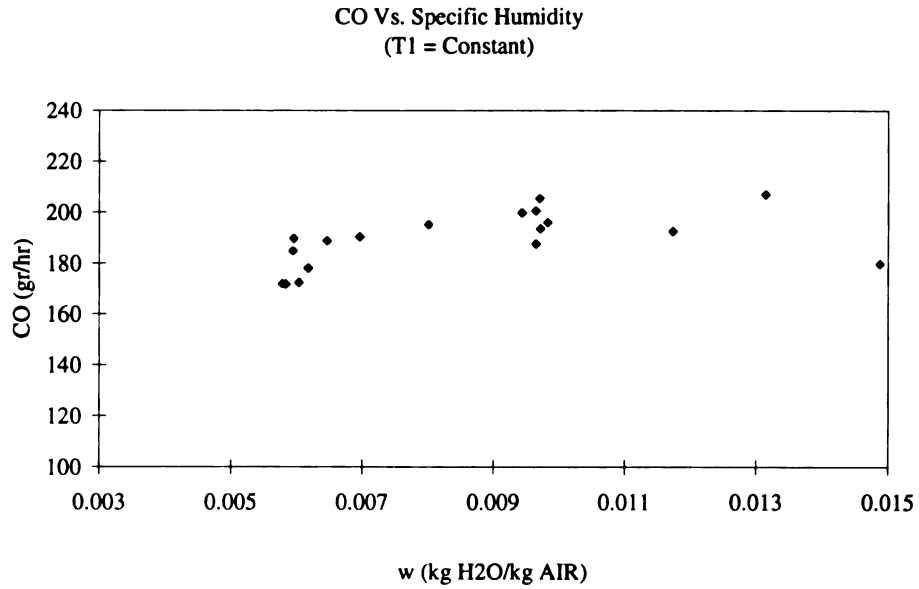


Figure 17: CO Vs. Specific Humidity

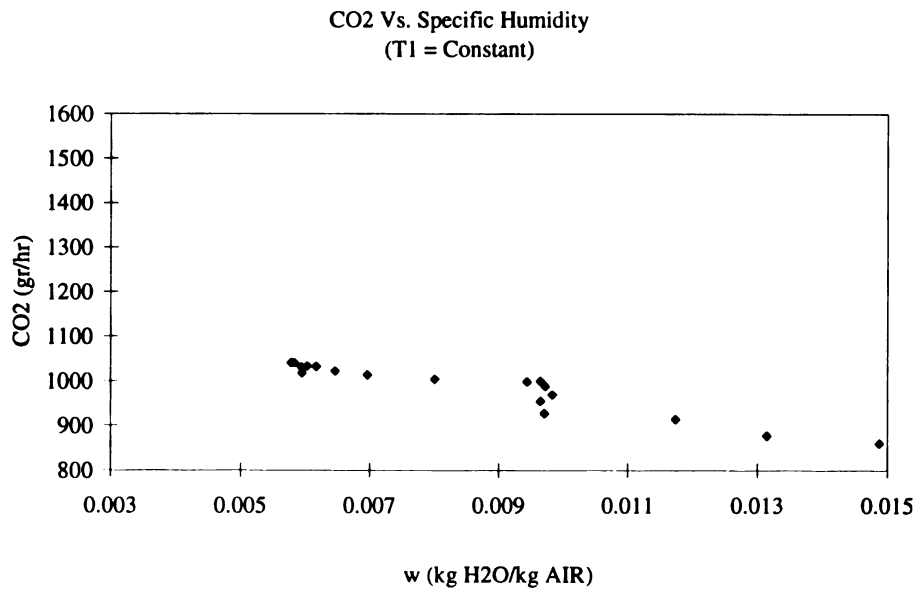


Figure 18: CO2 Vs. Specific Humidity

Finally the *HC* production is shown to increase drastically, from 21.73 (gr/hr) to 31.88 (gr/hr). This corresponds to a increase of 46.7%, over a humidity change of 0.01487 kg *AIR*/*H₂O* to 0.00578 kg *AIR*/*H₂O* (figure 20) The decreased *AFR* with ω is probably a contributing factor. Also the decreasing combustion temperatures are likely to result in lower exhaust gas temperatures, and possibly reduced post-exhaust oxidation.

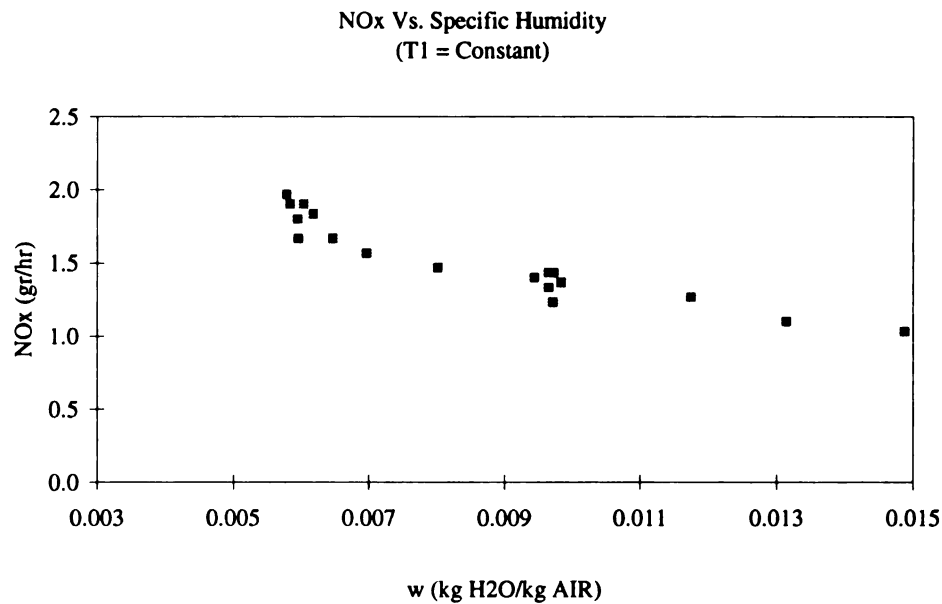


Figure 19: NOx Vs. Specific Humidity

Figure 21 shows the *AFR* versus the specific humidity. The *AFR* is shown to decrease as the humidity is increased. This minor change in *AFR* from 11.92 to 12.41 (3.95%) causes significant changes in the combustion products and process.

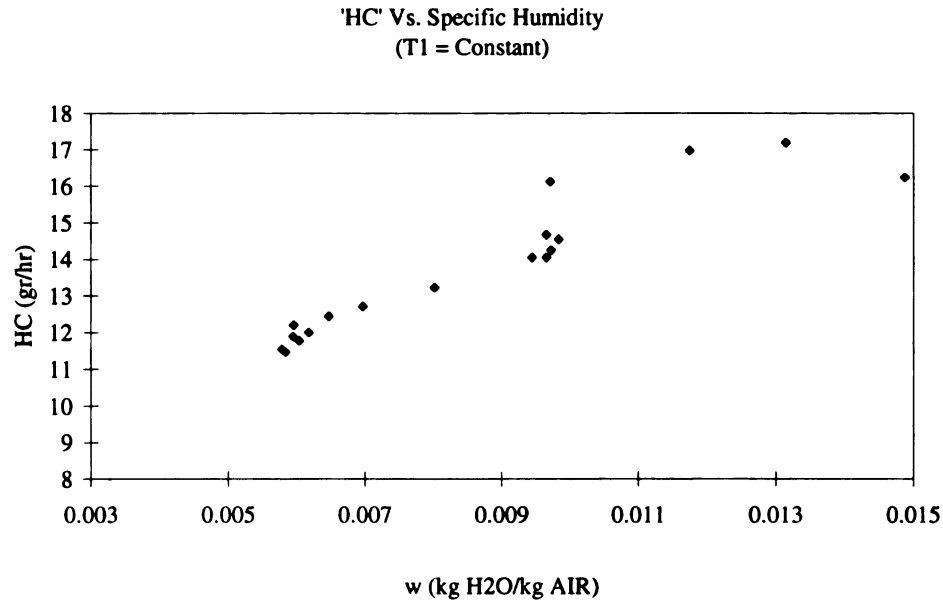


Figure 20: HC Vs. Specific Humidity

Lastly, figure 22 shows the ratio of CO/CO_2 as measured by the instruments (the diamond symbol) and the theoretical prediction (the square symbol). Here the AFR_d was set to 14.25 in order for the appropriate magnitudes to become similar. This is thought to arise from the compression model used. The ideal assumptions employed predicted combustion temperatures which are believed to be higher than the actual values (due to neglecting heat transfer). Since CO formation is extremely sensitive to combustion temperature [19], a slight reduction in temperature causes drastic decreases in CO production. In addition CO has been shown to increase with specific humidity, CO_2 must decrease with increasing specific humidity in order for the ratio of CO/CO_2 to increase. This trend is shown in the figure. CO increases with decreasing AFR , while CO_2 decreases with decreasing AFR .

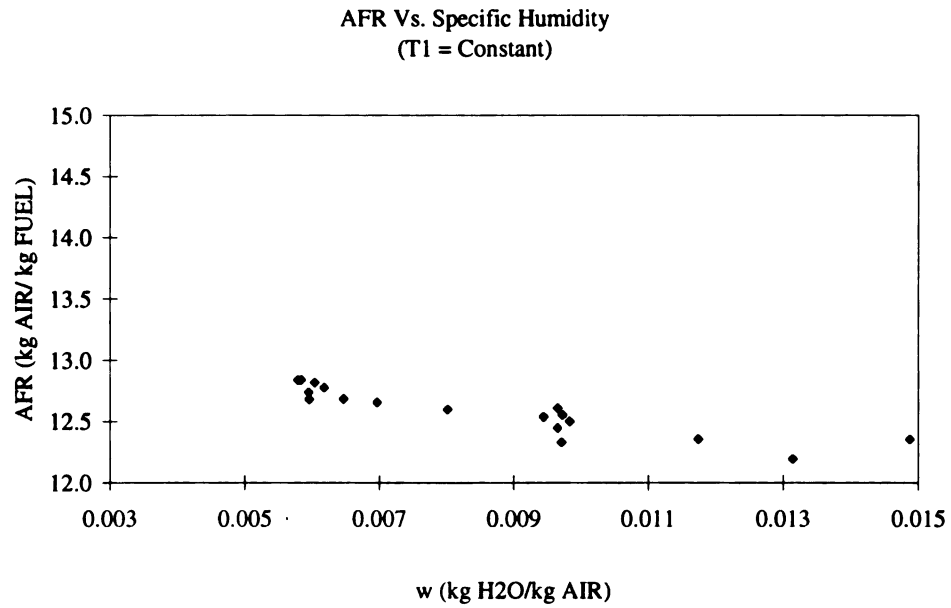
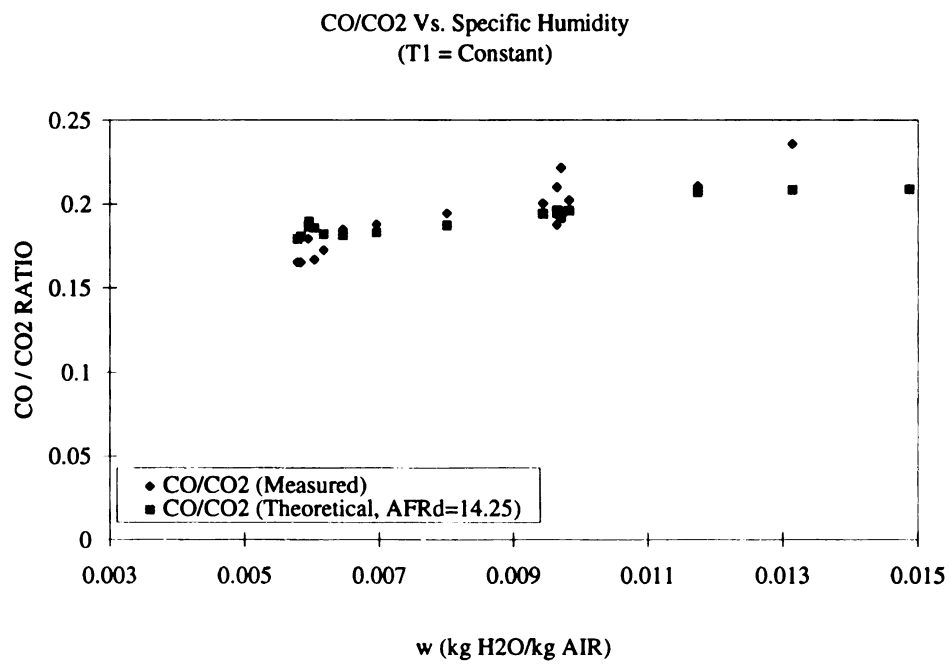


Figure 21: AFR Vs. Specific Humidity

Figure 22: CO/CO₂ Ratio Vs. Specific Humidity

3.3.2 Temperature Variation

The temperature variation proved to be a more difficult test to perform. The data has been truncated to include only the data that was maintained at constant humidity. As the room temperature was increased, the moisture level rose to the outside humidity value and leveled off. Thus it was hard to obtain strictly temperature dependent properties. Figure 23 illustrates the specific humidity dependence on temperature. This figure illustrates how the humidity value increased with increasing room temperature. The theoretical trend in AFR with T is restated below for convenience.

$$AFR_a = \frac{AFR_d}{\sqrt{(1 + \omega) \left(\frac{T}{T_{REF}} \right)}} \quad (14)$$

Engine torque is shown to decrease with increasing room temperature, as shown in figure 24. This is expected as the air is becoming less dense and the AFR is also decreasing (mixture is becoming richer). The richer mixture and the decreasing density of the air have a combined effect on engine performance. First the decreasing density of the air lessens the cylinder filling capabilities and second the decreasing AFR lowers combustion temperatures thus decreasing engine performance. The AFR decreases by a total of 1.96%.

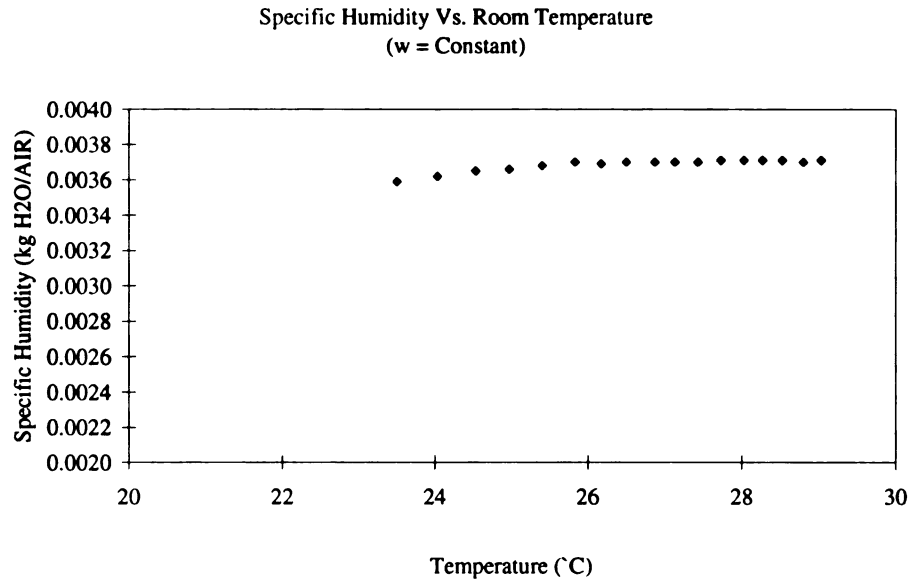


Figure 23: Specific Humidity Vs. Room Temperature

BSFC also varied with increasing room temperature as demonstrated with figure 25. BSFC decreased as a direct result of the decrease in engine torque (The *AFR* decreases by a total of 1.96%). With the *AFR* decreasing only slightly and the torque falling off significantly (torque decreased 17%), the BSFC has to increase. BSFC is a function of the fuel flow rate and power produced by the engine, as shown in equation 20.

The emissions also reflected the change in the surrounding temperature. *CO* production increased 25% with only a 1.96% decrease in the computed *AFR*. Figure 26 shows the *CO* as a function of room temperature. As the temperature becomes warmer, the mixture becomes richer, therefore more *CO* is produced (due to the lack of oxygen).

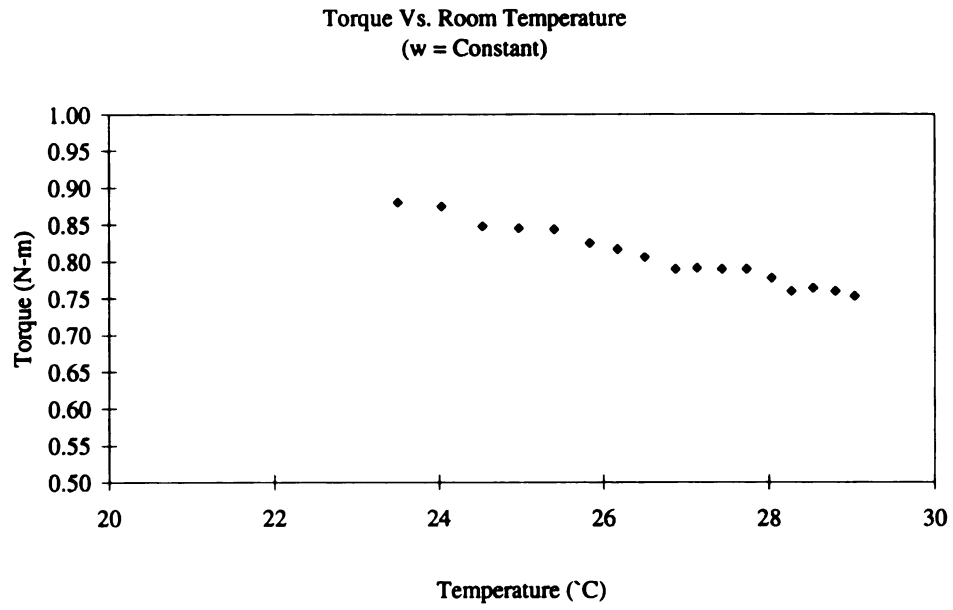


Figure 24: Engine Torque Vs. Room Temperature

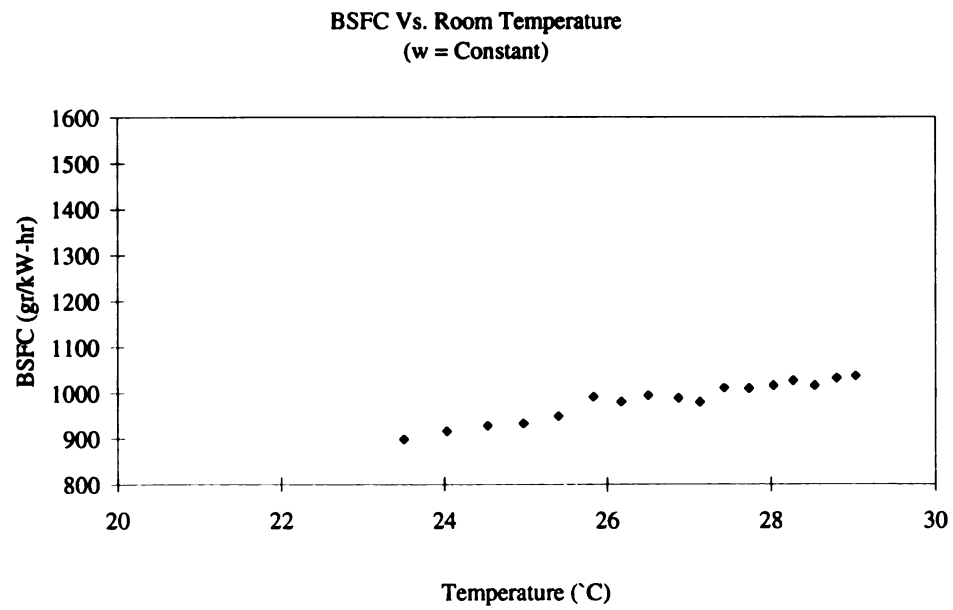


Figure 25: BSFC Vs. Room Temperature

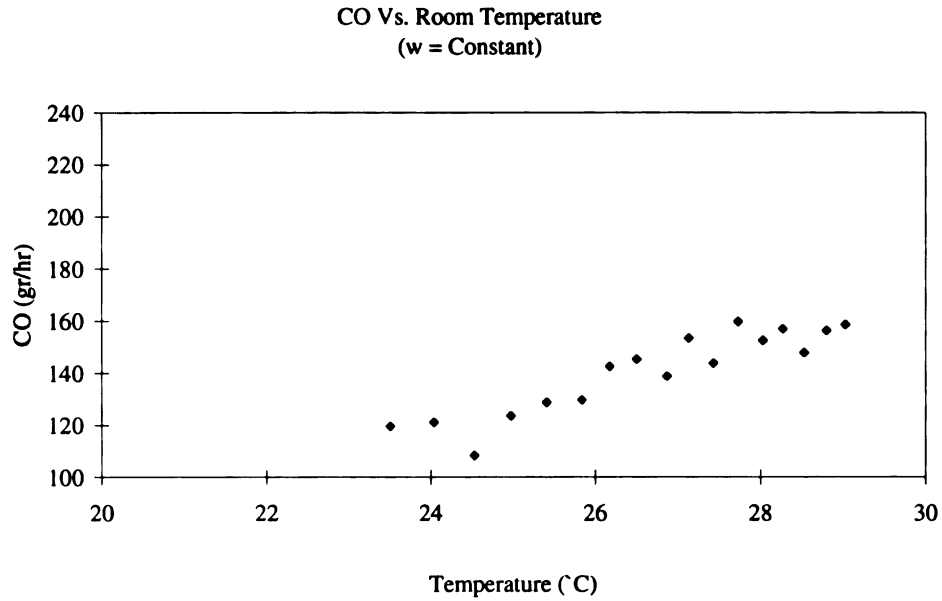


Figure 26: CO Vs. Room Temperature

The production of CO_2 was also effected by the changing ambient conditions. The production of CO_2 decreased with the increase in ambient conditions, as expected. With a decreasing AFR , the mixture becomes richer. As the mixture becomes richer, there is less oxygen available to produce CO_2 , so more CO is made. Figure 27 illustrates the decrease in CO_2 production.

Likewise, NO_x was similarly effected. Figure 28 shows NO_x as a function of the surrounding temperature. NO_x decreased 16.1%, but more resolution in the meter was needed. The span gas chosen was too rich, therefore the measured concentration shows step decreases as the room temperature is increased. Regardless of resolution, the NO_x decreased as a direct result of the decreasing AFR . The decrease in AFR results in lower combustion temperatures, thus less NO_x is produced.

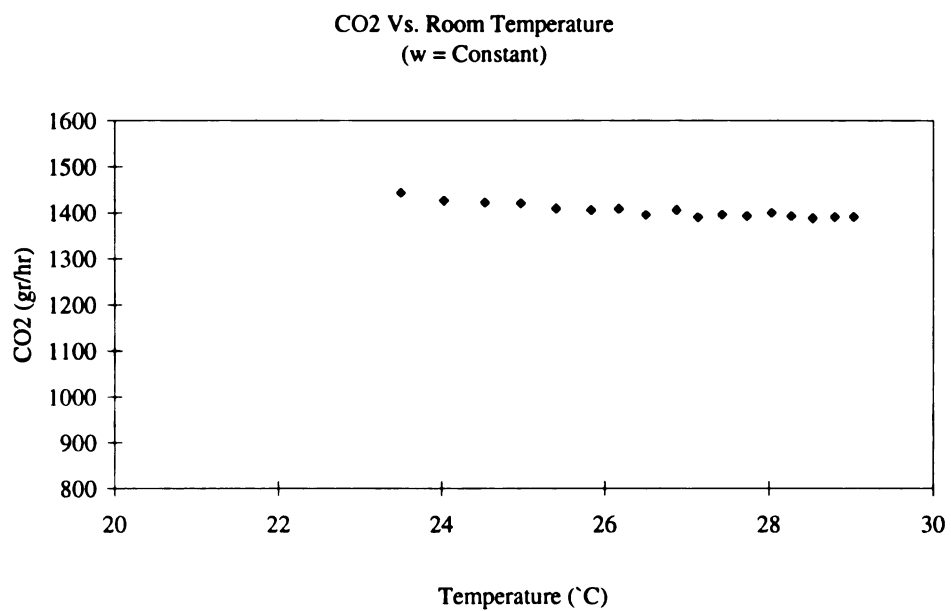


Figure 27: CO₂ Vs. Room Temperature

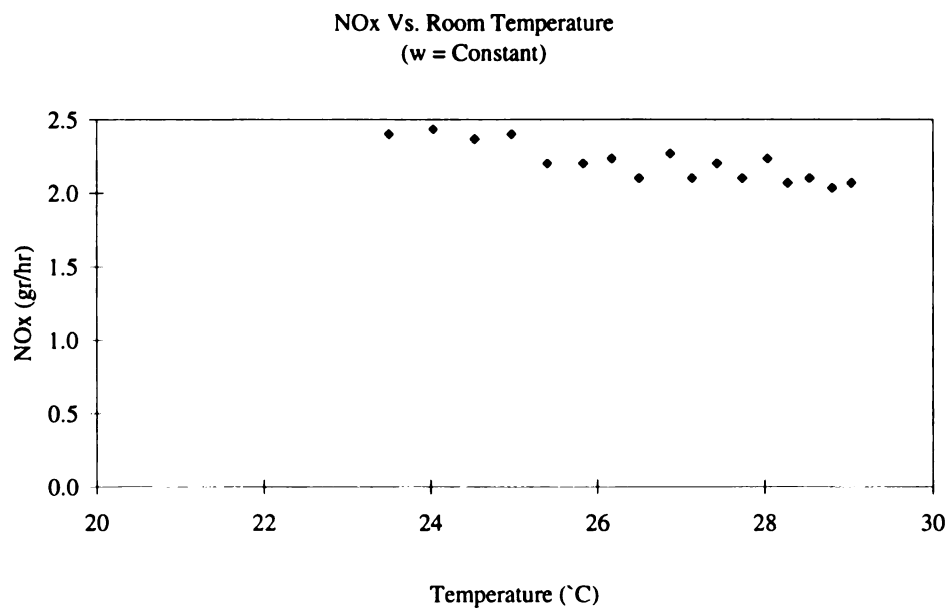


Figure 28: NO_x Vs. Room Temperature

HC production is illustrated in figure 29. The production of *HC* is not as drastic as the humidity change, never the less, the small decrease in *AFR* results in a small increase in *HC* production. This increase corresponds to a jump of 4.52%.

The *AFR* has already been discussed in some detail, but it is shown in figure 30. The *AFR* decreases only 1.96% over the testing range, but this rather minor change in *AFR* brings about modest changes in the emission levels produced by small engines in general.

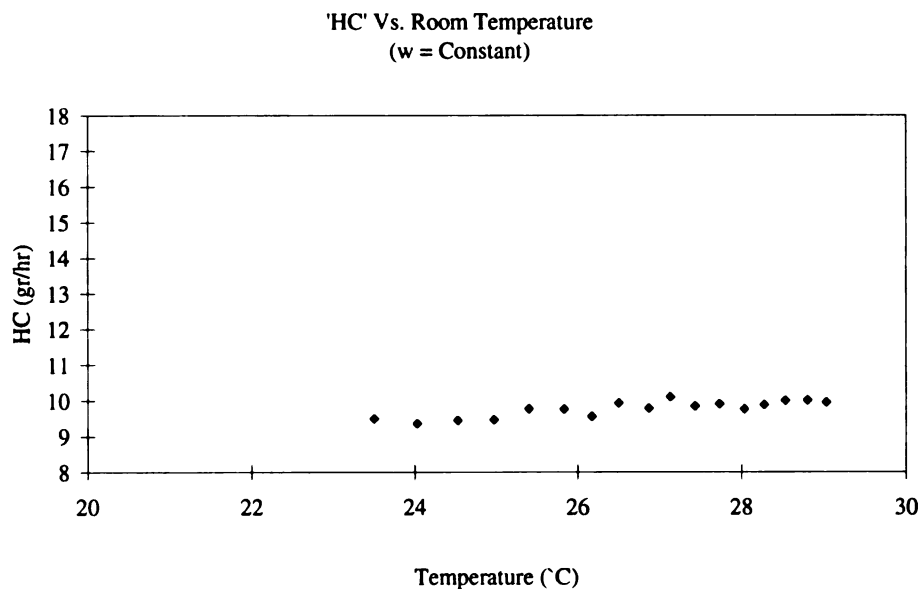


Figure 29: HC Vs. Room Temperature

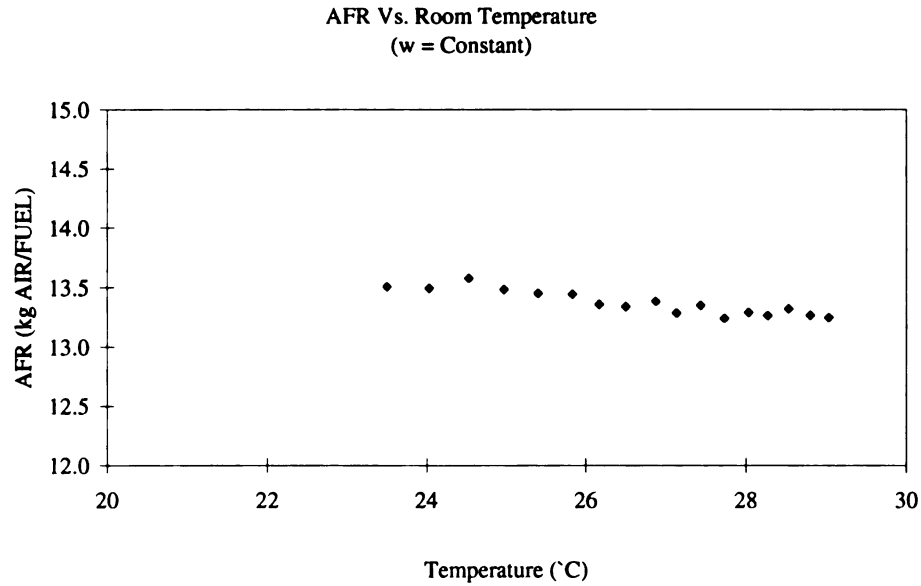


Figure 30: *AFR* Vs. Room Temperature

Finally the measured CO/CO_2 ratio (diamond symbols) is compared to the theoretical results (square symbols). This is shown in figure 31. The AFR_d had to be raised to 14.25 in order for the magnitudes to be nearly identical. Again, this is thought to arise from the compression model used. The ideal assumptions employed predicted combustion temperatures which are believed to be higher than the actual values (due to neglecting heat transfer). Since CO formation is extremely sensitive to temperature, a slight reduction in temperature causes drastic decreases in CO production. The ambient temperature change is thought to bring about more effects than just changes in ambient energy levels. It is known to be responsible for fuel evaporation rates, heat transfer from the engine, air density and others.

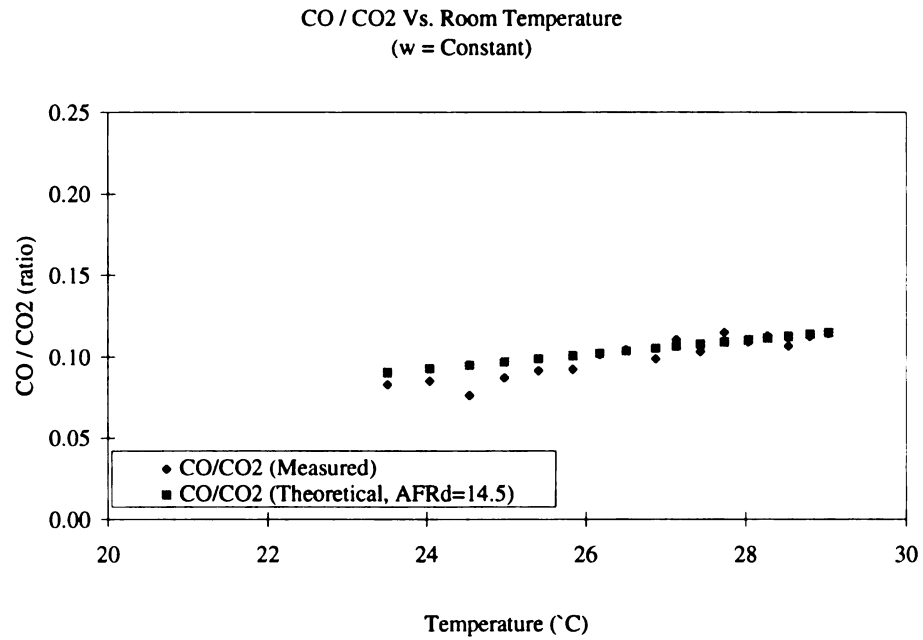


Figure 31: CO/CO₂ Ratio Vs. Room Temperature

4. CONCLUSIONS

- 1) In general, changes in ambient conditions lead to small changes in the actual *AFR* in carbureted IC engines. These *AFR* changes produced modest changes in measured emission levels. However, the effect of ambient humidity on flame temperature is particularly large. For example a 1.96% increase in *AFR_a* (becoming leaner) resulted in a 50% increase in *NO_x* production.
- 2) The performance and emissions measurements: *BSFC*; *CO*; *CO₂*; *NO_x*; *AFR* and *CO/CO₂* ratio all exhibited clear trends with changes in ambient conditions. Increasing specific humidity or temperature caused an increase in *BSFC*, *CO* and, *CO/CO₂* while reducing *CO₂*, *NO_x* and *AFR*.
- 3) *CO/CO₂* formulations are highly temperature and *AFR* dependent therefore they are difficult to predict from theory. Since the isentropic compression model was assumed not to include any heat transfer from the charge, this estimate of the compressed charge temperature is probably higher than its actual value. Selecting the lower limit at which equilibrium thermodynamics applies appears to be 1700 K (Spindt [8], Heywood [19]). This leads to a reasonable agreement with experimental results.
- 4) Changes in ambient temperature not only effect air density, but also fuel evaporation rates, heat transfer from the engine and compression properties. In contrast changes in humidity seen only to affect the charge composition and

its properties. Therefore effects of changing ambient temperature on emissions are potentially much more complex than changing humidity.

- 5) More research may be needed in the area, in order to better understand how changes in ambient humidity and temperature effect engine performance.

Appendix A

Appendix A

Apparatus

A.1 Fuel Flow Measurement

The fuel flow cart uses a Micro-Motion mass flow meter. This meter operates using the Coriolis effect. The flow tubes of the Coriolis mass flow sensor are driven at their natural frequency by a magnet and drive coil attached to the center of the bent u-tube, see figure 32. The vibrating motion of the u-tube, combined with the momentum of the fluid flowing within the tube, induces a Coriolis force that causes each flow tube to twist in proportion to the rate of mass flow through the tube during each vibrational cycle, see figure 33. Since one leg of the flow tube lags behind the other leg during this twisting motion, the signals from sensors on the two tube legs can be compared electronically to determine the amount of twist, see figure 34. The transmitter measures the time delay between the left and right pickoff signals using precision circuitry and a high frequency crystal controlled clock. This delta time value is multiplied by the flow calibration factor to determine the mass flow rate then the resulting flow rate is displayed by the Digital Rate Totalizer (DRT) and sent to the PC [24]. Other sensors on the flow cart measure the temperature and relative humidity within the room and this data is also sent to the PC for “storage”. See Figure 35 for a fuel flow schematic. After the fuel leaves the flow cart, it is sent to the carburetor.

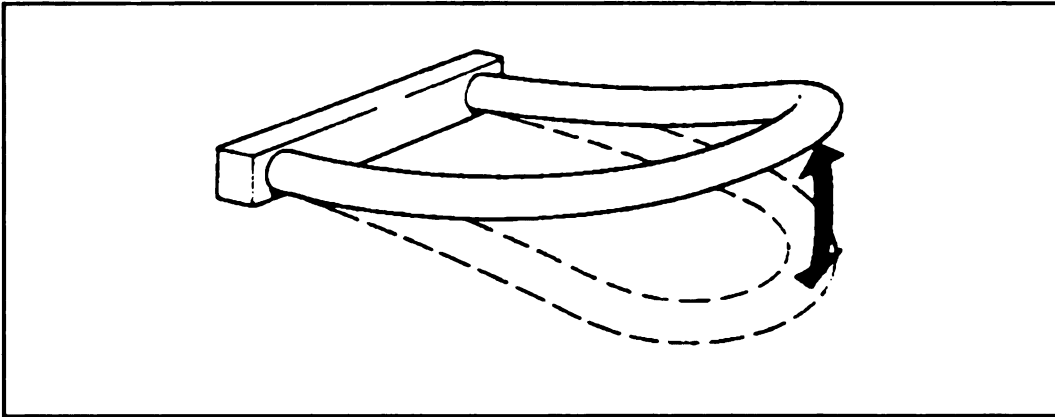


Figure 32: Vibrating flow tube (single flow tube shown)

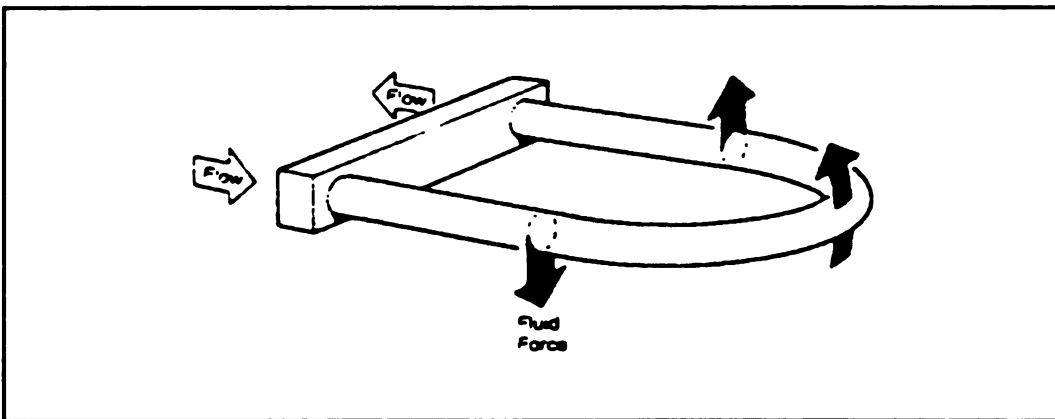


Figure 33: Fluid Forces Reacting in Vibration of Flow Tube

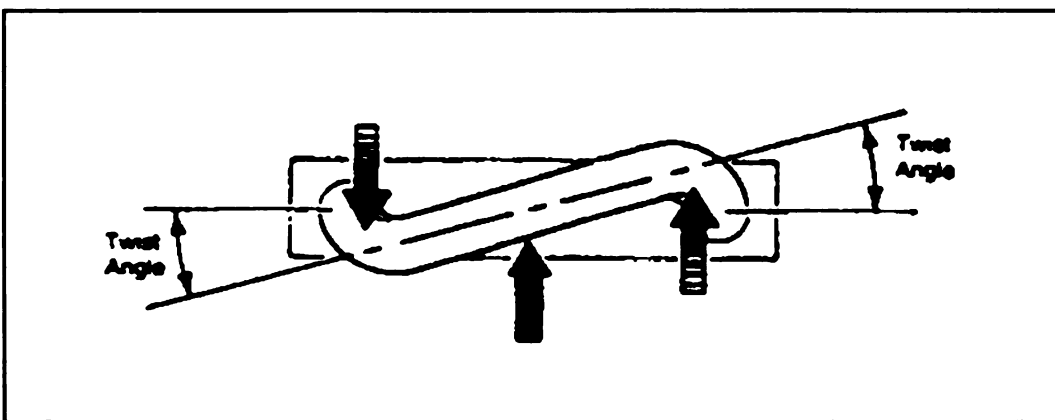


Figure 34: End View of Flow Tube Showing Twist

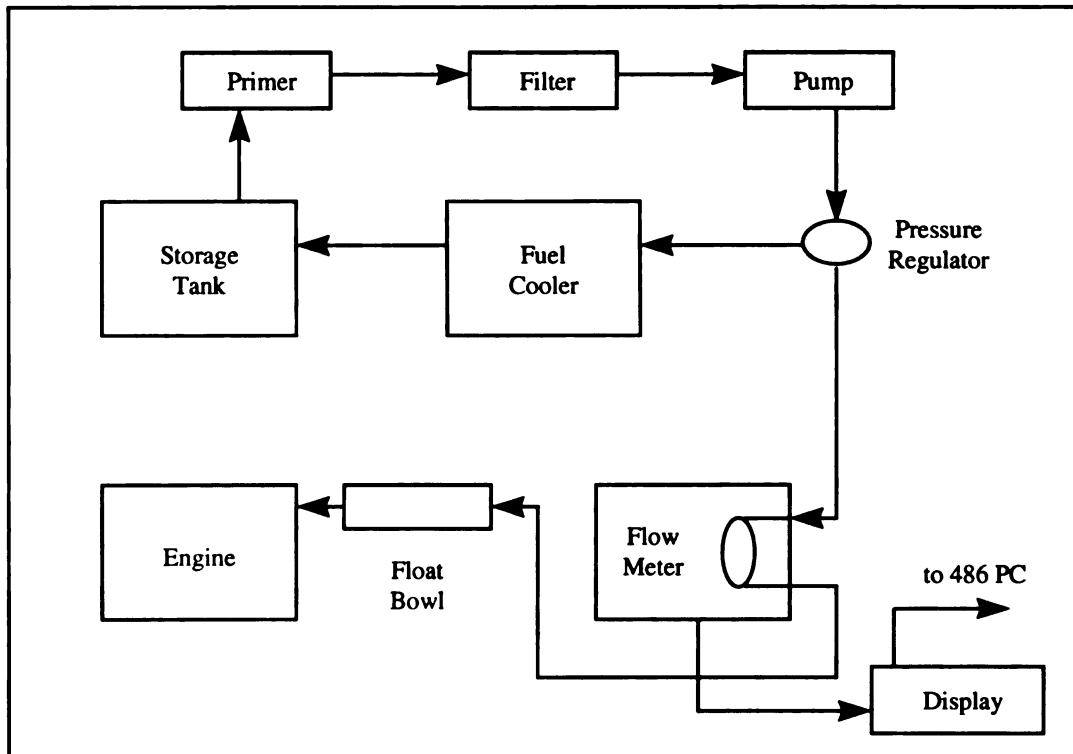


Figure 35: Fuel Flow Cart

A.2 Dynamometer and Controls

The dynamometer measures various engine operating parameters, including engine torque, engine RPM, cylinder head temperature, exhaust temperature, oil temperature and fuel temperature. The dynamometer is a Micro-Dyn model 15, which is capable of dissipating approximately 20.4 N-m (15 ft-lbs) of torque. The maximum engine operating speed for this dynamometer is 14,000 rpm. It is a low inertia, hydraulic dynamometer which dissipates the energy produced by the engine through an oil to air heat exchanger. The dynamometer is computer controlled, with settings for speed, throttle opening or other test operating conditions (such as transient operation). It uses a hydraulic pump driven by an electric motor as the working fluid. The fluid flow rate is controlled by the computer via a stepper motor, which governs the engine RPM (figure 36

shows a fluid flow schematic). With the RPM set by the flow rate, one is ready to load the engine, by setting the throttle opening to the desired setting. In between the engine and hydraulic pump is the torque sensor, a Lebow model 1804-500. This torque meter measures the torque output from the engine, and sends the appropriate electrical signal to the computer. The torque output from the engine can be displayed either as the instantaneous torque through one engine cycle, or as an integrated “mean” torque using an RC circuit.

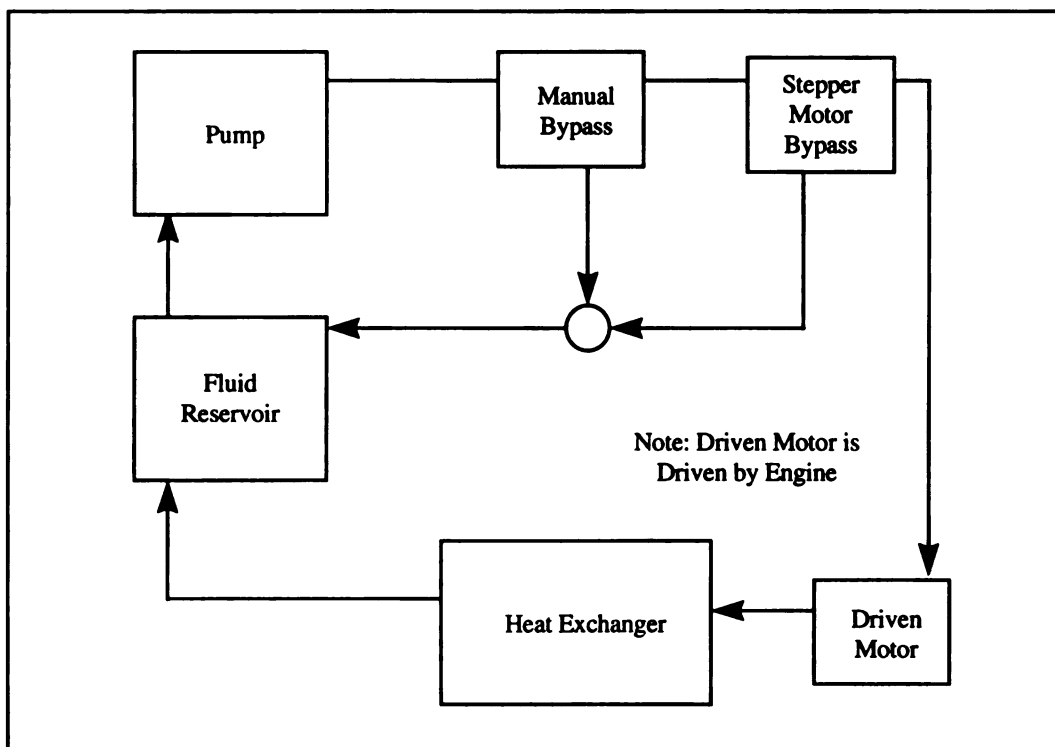


Figure 36: Dynamometer Hydraulic Circuit

A.3 Environmental Controls

The temperature and humidity within the room were monitored and controlled by a set of Honeywell Industrial controls. These controls were specifically designed for this purpose. A Honeywell model T775-E controls the humidity within the room while a Honeywell model T775-A monitors the temperature. They are connected to a steam generator, a heating unit and a refrigeration unit. See figure 37 for a schematic.

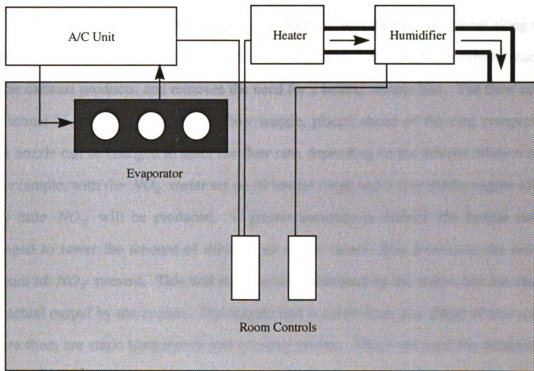


Figure 37: Temperature and Humidity Controls

A.4 Dilution Tunnel

The dilution tunnel consists of a 4" diameter pipe, an air bleed valve (which allows excess air to be drawn into the compressor, assuming the nozzle has a smaller flow rate than the compressor), a nozzle and a ring compressor. There is also a secondary air inlet valve, down stream of the primary air inlet valve, to adjust the suction that is imposed on the exhaust exit. Some engines are susceptible to decreases in exhaust exit pressure and hence the performance can be altered if this is the case.

When the exhaust leaves the engine, it is drawn into the dilution tunnel along with large quantities of room air. The effect of this dilution is to freeze any further reaction by the exhaust products, and removes the need for a heated sample line. The flow rate in the tunnel is governed by a critical flow nozzle, placed ahead of the ring compressor. This nozzle can be changed to tailor the flow rate, depending on the desired dilution ratio. For example, with the NO_x meter set on its lowest range and a four stroke engine idling, very little NO_x will be produced. If greater accuracy is desired, the nozzle can be changed to lower the amount of dilution air in the tunnel, thus increasing the relative amount of NO_x present. This will increase the value read by the meter, but not change the actual output by the engine. The sample line is taken from just ahead of this nozzle where there are static temperature and pressure probes. These are used for determining the flow rate, using Bernoulli's equation. After the exhaust gases pass through the ring compressor, they are sent through an exhaust duct, and expelled to the atmosphere (see Figure 38).

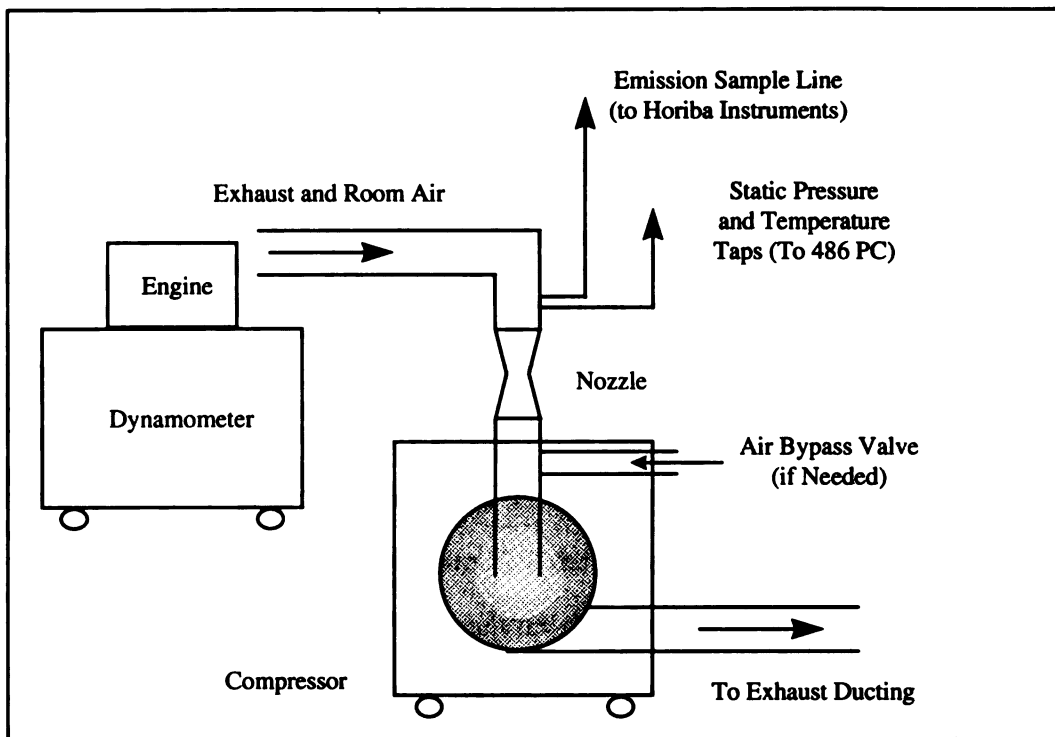


Figure 38: Dillution Tunnel

A.5 Emission Measurement

With the sample coming from just ahead of the critical flow nozzle, after the exhaust mixture has traveled through the exhaust tubing for almost 15 feet, one can assume it is well mixed. The sample line takes a small sample and pipes it over to the Horiba Bag Bench. Each analyzer measures the species of interest using a different principle, measuring each constituent as a volume fraction of the total exhaust gas sample. The CO and CO_2 meters, employ a non-destructive measurement technique. This involves passing specific wavelength of infra-red light (IR) through the sample (see figure 39). An IR detector on the opposing side, detects how much IR light has passed through the sample. Since CO and CO_2 absorb IR light (over different frequency ranges), the greater the concentration of CO or CO_2 in the sample, the less IR light will

pass through. From the Amagat model of ideal gases, the volume fraction is proportional to the mole fraction present, and therefore the volume fractions of CO and CO_2 can be found.

The HC meter uses a different approach and is “tuned” to specific carbon compositions within the species. For example, the composition of two stroke exhaust mirrors the composition of the two stroke fuel. On the other hand, the composition of four stroke exhaust, is mostly composed of C_1 and C_2 molecules [6]. Therefore one must use a span gas, that closely resembles the exhaust gas in question. If this is not done, false readings can result. The analyzer detects the amount of HC 's present in the sample using the flame ionization technique. The flow of a sample with carbon compounds through a hot flame leads to ionization of the gas and an ionization current. This current is proportional to the volume fraction of HC 's present within the sample.

The NO_x meter uses a chemical illumescent process. Nitrogen compounds in the exhaust gas are actually a mixture of NO and NO_2 , which is usually written as NO_x . In the analyzer, the NO_2 is first converted to NO . The resulting sample then reacts with O_3 , which is generated by an electrical discharge through oxygen, at a low pressure in a heated vacuum chamber. The light emitted by the reaction is measured by a photomultiplier and indicates the NO_x concentration within the sample. NO and NO_2 are not stable at room temperature. It is for this reason we refer to them simply as NO_x . If one takes and measures a sample of NO and NO_2 and places it in a bag for storage, the concentrations of each species will change with time and temperature. See table 5 for an overview of the emission measurement techniques.

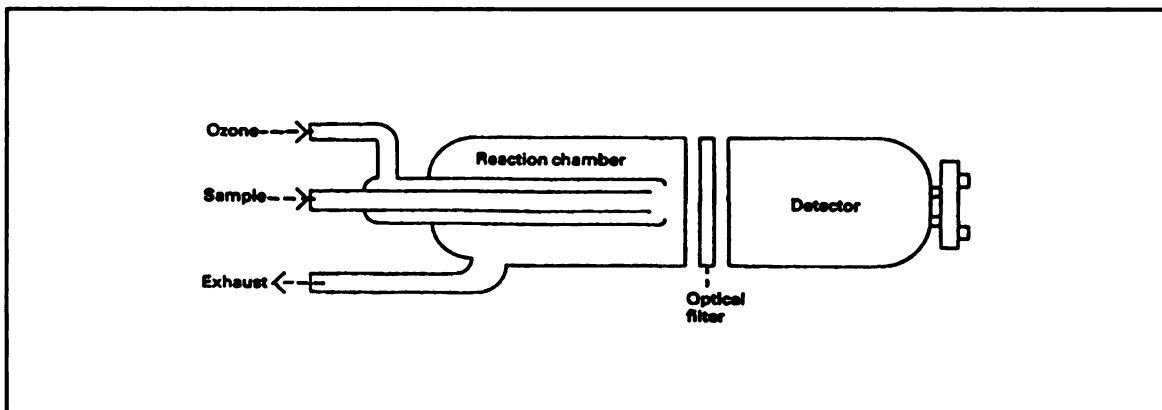
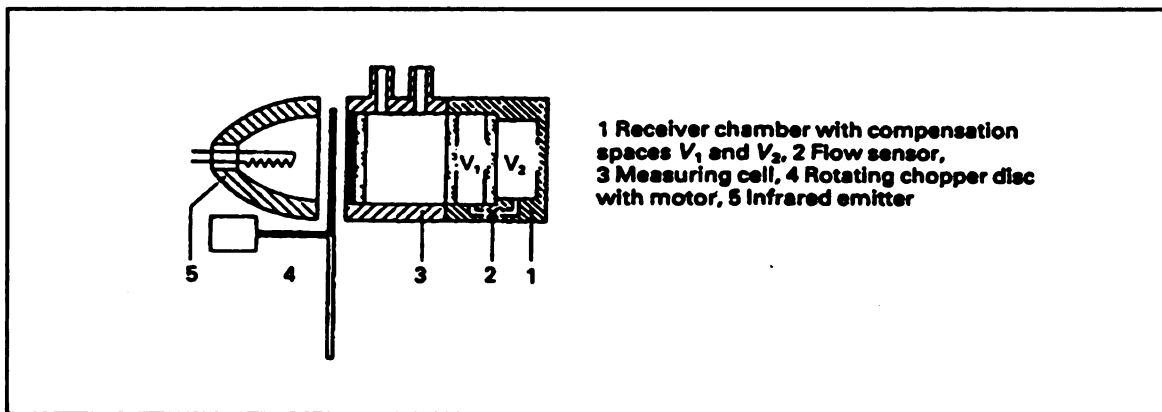
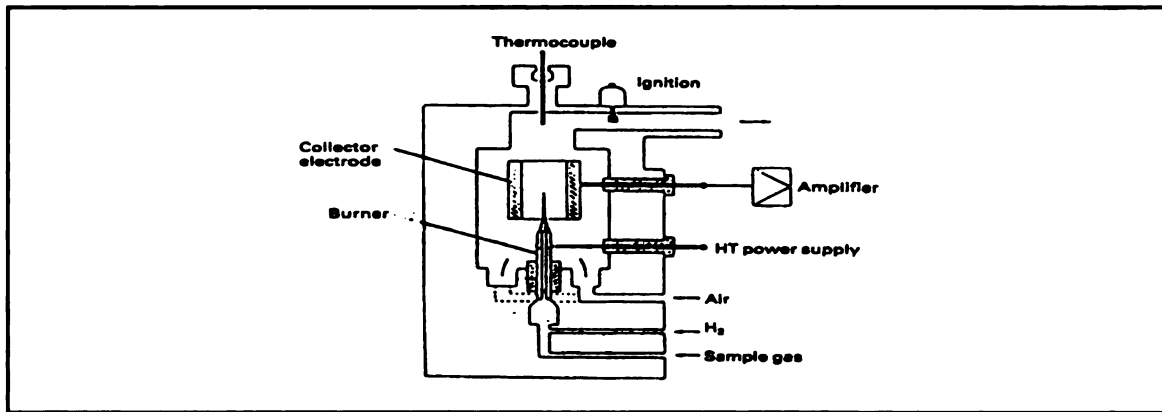


Figure 39: Analyzer Cross Sections

From Top to Bottom: Flame Ionization Detector, Non Dispersive Infra-Red Analyzer and Chemiluminescence Detector

Table 6: Emission Measurement Techniques

| GAS | TECHNIQUE | TYPICAL RANGE |
|------------------------------|---------------------------------|---------------|
| CO | Non dispersive Infra Red (NDIR) | 0-3000 ppm |
| CO ₂ | Non dispersive Infra Red (NDIR) | 0-20 % |
| NO _x | Chemiluminescence | 1-10,000 ppm |
| UNBURNED HYDROCARBONS (HC's) | Flame Ionization Detector (FID) | 1-10,000 ppm |

A.6 Data Collection

After all the components are measured, the resulting voltages are digitized through one of three Data Translation digital to analog (D/A) boards. The IBM 486 PC uses two voltage conversion boards and one thermocouple board for reading all the pertinent room data to the FORTRAN code for analysis (see figure 40). In addition to these three D/A boards, the fuel flow cart transmits its data through an RS-232 serial port into the IBM 486 PC. Next, the program SAMPLE takes ten samples of each value in question, and uses the average to calculate a single data point. Then SAMPLE is run two more times to obtain two more data sets, again each one is an average over ten individual samplings. Convert was written to read in all the data values outputted from our program SAMPLE. This code read in the raw data (in table form) took the *average* for three data points, and output the data (in column form) to a specified file name. The average of all three results represents one data point in my data. See figure 41 for clarification.

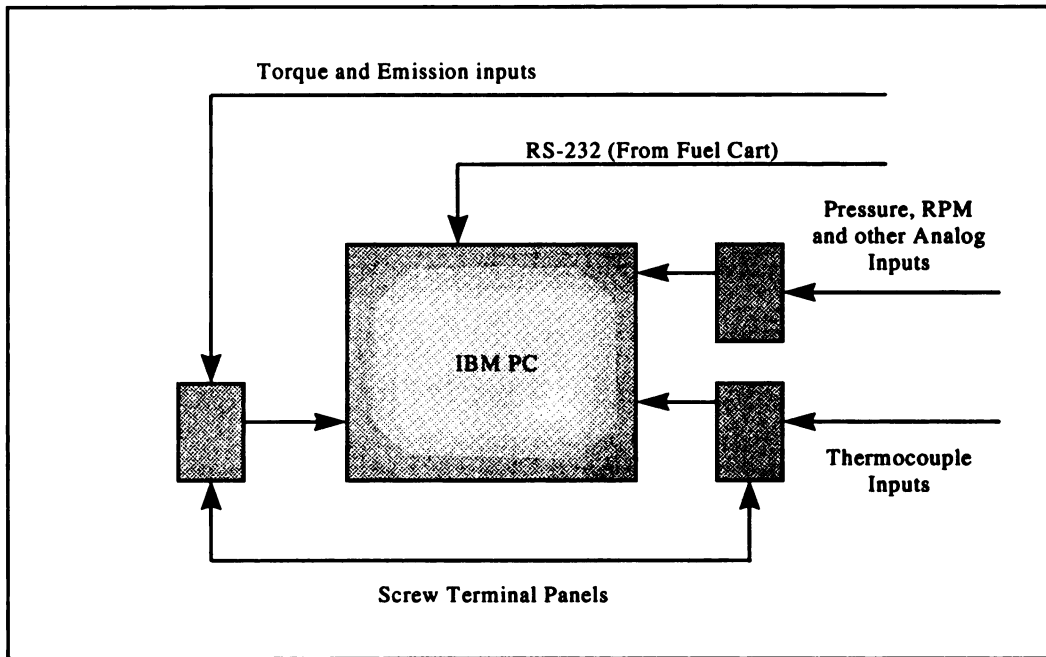


Figure 40: Data Collecting Computer (486 PC)

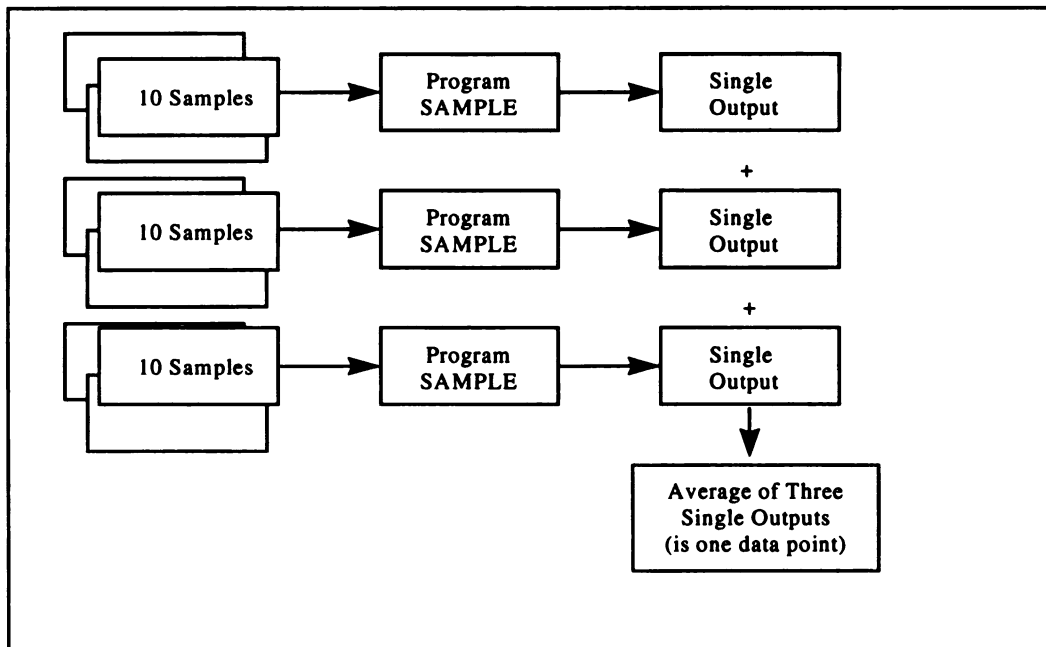


Figure 41: Data Collecting Algorithm

Appendix B

Appendix B

Scaling Analysis

In order to verify or check the constant U , constant ν assumption, a scaling analysis of the first law will be performed.

From the first law,

$$dQ - dW = dE \quad (14)$$

Dividing by the change in Gibbs free energy,

$$\frac{dQ}{\Delta G} - \frac{dW}{\Delta G} = \frac{dE}{\Delta G} \quad (22)$$

Each term in equation (22) must be estimated, and the relative magnitudes are then compared.

B.1 Heat Transfer

Starting with the heat transfer, dQ , which is estimated using a Woshni [15], [16] correlation. Starting with the basic heat transfer equation,

$$q_w = hA(T_w - T)$$

a sensible estimation for the heat transfer coefficient (h) is as follows,

$$h = 0.0032 P^{0.8} \frac{(V_{MOT} + V_{COMB})^{0.8}}{B^{0.2} T^{0.53}}$$

where,

$$V_{MOT} = C_1 V_{PISTON}$$

$$V_{COMB} = C_2 \frac{V_d T_1}{P_1 V_1} (P - P_{MOT})$$

C_1 and C_2 are constants, and given in the following table,

Table 7: Table of Woshni Coefficients

| | Compression | Combustion - Expansion |
|-------|-------------|------------------------|
| C_1 | 2.28 | 2.28 |
| C_2 | 0.00 | 0.00324 |

The average piston speed is V_{PISTON} and is defined by, $Stroke/Time$. V_d is the displacement volume, T_1 , P_1 and V_1 are evaluated at a reference condition, say inlet valve

closing. P is the cylinder pressure and P_{MOT} is the pressure under motoring conditions. P_{MOT} , is assumed to be the pressure at the end of compression. B is the cylinder bore and T is the cylinder temperature. The total heat transfer is estimated to be 391.7223 J / kg .

B.2 Work

Work in and out of the engine during the compression / expansion process is assumed to follow the integral:

$$W = \int_1^2 P dV \quad (23)$$

The combustion is assumed to occur over a finite period of time, or a specific amount of crank angle degrees. Heywood, [19] estimates for rich mixtures, the combustion rate is higher than for lean mixtures. Small engines are set to run on the rich side, and therefore the crank angle needed for combustion is assumed to be 50° (pp. 382, figure 9-8-a). A schematic of a P - v diagram is included below (figure 42). The net work out, W_{net} , is the total area under the curve, or

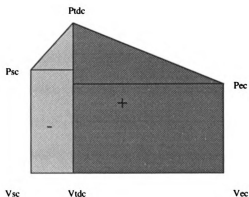


Figure 42: Work inputs and outputs

Where the Subscripts in the picture are defined as following:

1. P - Pressure
2. V - Volume
3. sc - Start of Combustion
4. tdc - Top Dead Center
5. ec - End of Combustion

V_{sc} is point 1, V_{ec} is point 2. The pressure change is assumed to be polytropic, so the pressure rise follows the equation:

$$(Pv)^{\frac{C_p}{C_v}} = \text{CONSTANT} \quad (24)$$

Since the peak pressure is known, the pressure at start of combustion can be backed out using an estimated volume (specified crank angle). Likewise the end of combustion pressure can also be found. With the pressures and volumes known, the work input (piston is moving upwards, pressure is rising) and the work output (piston is moving down, pressure is falling) can be found. The figure illustrates the work output is much larger than the work input, as it should be.

The displacement was found using the physical engine parameters and a relation found in Taylor [17]. The swept volume is a function of cylinder bore, stroke and rod length. The stroke length prior to TDC was estimated as 0.00049635 m and that after TDC was 0.00373235 m, assuming a total combustion time of 0.00119 seconds (50 crank degrees @ 7000 RPM).

With these assumptions and equations, the work input during the combustion process was estimated to be 299.144 J/kg , the work out during the combustion / expansion was estimated to be 510.529 J/kg , so the net work, W_{net} , is the difference of the two, or 211.38 J/kg .

B.3 Internal Energy

The internal energy of the system, $E (= U)$ is assumed to be constant throughout the combustion process. Therefore the *RHS* of the first law (equation 22) is zero.

B.4 Change in Gibbs Free Energy

Gibbs free energy is defined to be:

$$G = H - TS \quad (25)$$

and H is $U + PV$. Substituting into (25)

$$G = U + PV - TS \quad (26)$$

The change in Gibbs free energy is the difference between two points or,

$$\Delta G = G_1 - G_2 \quad (27)$$

Since $U_2 = U_1$ and $V_2 = V_1$, the difference in the free energy is:

$$\Delta G = (P_1 V_1 - T_1 S_1) - (P_2 V_2 - T_2 S_2)$$

since the volume ratios are the same, the above reduces to,

$$\Delta G = (P_1 - P_2) \mathcal{V} - T_1 S_1 + T_2 S_2 \quad (28)$$

From combustion analysis [14],

1. $P_1 = 1.5189 \text{ e6 } Pa$
2. $P_2 = 8.6444 \text{ e6 } Pa$
3. $T_1 = 549.69 \text{ K}$
4. $T_2 = 2883.87 \text{ K}$
5. $S_1 = 6.6596 \text{ e3 } J / kg - K$
6. $S_2 = 8.7624 \text{ e3 } J / kg - K$

The change in Gibbs free energy, ΔG , is estimated as $2.0903 \text{ e7 } J / kg$.

From (22), substituting in the appropriate values:

$$\frac{dQ}{\Delta G} - \frac{dW}{\Delta G} = 0$$

$$\frac{391}{2.09e7} - \frac{211}{2.09e7} \cong 0$$

This shows that our constant U , constant v assumption is valid.

Appendix C

Appendix C

Compressibility Estimation

In order to neglect the effects of compressibility through the carburetor throat, they must not contribute a significant part to the flow equation. Heywood [19] states: “For flow rates less than about 60 percent of the choked flow, the effects of compressibility on the mass flow rate are less than 5 percent (pp. 909).”

Choked flow is defined as flow when the Mach number is equal to one, or

$$\hat{M} = \frac{V}{c} = 1 \quad (29)$$

where \hat{M} is the Mach number, c is the speed of sound and V is the observed velocity. If the Mach number is equal to 1, $V = c$. From:

$$\dot{m} = \rho A V \quad (30)$$

The velocity of air through the orifice can be found. Assuming 100% volumetric efficiency (worst case), a four stroke engine takes in its displacement in air every other revolution, or,

$$7000 \frac{rev}{min} \left(\frac{1 charge}{2 rev} \right) = 3500 \frac{charge}{min} \left(\frac{1 min}{60 sec} \right) \left(\frac{26 cm^3}{charge} \right) = 1516 \frac{cm^3}{sec}$$

$$1516 \frac{cm^3}{sec} \left(\frac{1 m}{100 cm} \right)^3 = 0.001517 \frac{m^3}{sec} \quad (31)$$

Equation (31) is the volume flow rate of air through the venturi, assuming 100% volumetric efficiency, and only dry air flowing through the restriction. In order to obtain the velocity, divide the volume flow rate by the area it is flowing through,

$$V = \frac{\dot{m}}{\rho A} = \frac{\rho \dot{V}}{\rho A} = \frac{\dot{V}}{A} \quad (32)$$

or,

$$\frac{0.001517 m^3/sec}{2.8257e-5 m^2} = 53.631 \frac{m}{sec}.$$

In terms of the Mach number,

$$\hat{M} = \frac{V}{c} = \frac{53.631}{343.3} = 0.15622$$

or 15.6%. Heywood states the effects of compressibility are only relevant when the Mach number is about 60%, so the effects of compressibility are neglected in this study. Mach number value from Munson, Young and Okiishi, table B-4, pp. 809 [20].

Appendix D

Appendix D

Equilibrium Calculations

Consider a general chemical reaction equation [19]:

$$y_a M_a + y_b M_b + \dots = y_l M_l + y_m M_m + \dots \quad (33)$$

This can be re-written as:

$$\sum_i y_i M_i = 0 \quad (34)$$

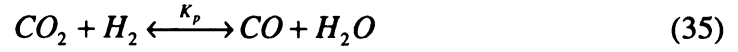
which leads to,

$$\sum \ln \left(\frac{P}{P_o} \right)^{y_i} = - \frac{\Delta G^o}{RT} = \ln K_p$$

Where K_p is the equilibrium constant at constant pressure, P is the operating pressure and P_o is a reference pressure. The equilibrium constant for a given reaction is then obtained from the equation:

$$K_p = \frac{[y_l][y_m]}{[y_a][y_b]}$$

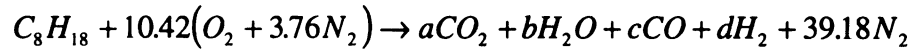
For fuel rich combustion, the equilibrium of CO and CO_2 during expansion and the subsequent exhaust processes is often assumed to follow the “water-gas” reaction [19] [8]:



with the equilibrium constant defined as,

$$K_p = \frac{[CO][H_2O]}{[CO_2][H_2]}.$$

For an AFR of 12.5,



A Carbon balance yields: $a + c = 8$

A Hydrogen balance yields: $2b + 2d = 18$

An Oxygen balance yields: $2a + b + c = 20.83$

In addition the equilibrium states $(bc)/(ad) = 3.388 = K_p$. These four equations can be solved to obtain,

$$c^2 - 19.3c + 47.3 = 0 \quad (36)$$

which gives $c = 2.89$, $a = 5.12$, $b = 7.72$, and $d = 1.29$. The total number of moles are found by summing the parts, or $a + b + c + d + 39.3 = 56.3$, so the mole fractions are: $CO_2 = 0.0908$; $H_2O = 0.137$; $CO = 0.051$; $H_2 = 0.023$ and $N_2 = 0.698$. This procedure can be expanded to include moist air. Equation (14), restated below for convenience, states that the actual AFR (AFR_a) is a function of the design AFR (AFR_d), temperature and humidity.

$$AFR_a = \frac{AFR_d}{\sqrt{(1 + \omega) \left(\frac{T}{T_{REF}} \right)}} \quad (14)$$

Thus, the theoretical CO / CO_2 ratio can be found for different AFR_d , temperatures and humidities.

Appendix E

Appendix E

Measured Quantities

Below is an output file from the program SAMPLE. These are the measured and calculated quantities.

| <u>Emissions</u> | | <u>Operating Conditions</u> | | <u>Temperatures</u> | |
|-----------------------|--------|-----------------------------|--------|---------------------|-------|
| Fuel flow (gr/hr) | 524.7 | Speed (rpm) | 6797. | T_nozzle(^C) | 21.4 |
| HC(C_1) (ppm) | 0.2220 | Power (brake kW) | 0.4819 | T_cyl (^C) | 161.5 |
| NO _x (ppm) | 0.0587 | Torque (N-m) | 0.6766 | T_exhaust (^C) | 249.1 |
| CO ₂ (%) | 0.4009 | Rel. Humidity (%) | 62.25 | T_fuel (^C) | 20.0 |
| CO (ppm) | 0.2604 | P_diff (kPa) | 0.122 | T_room (^C) | 12.9 |
| CH ₄ (ppm) | 0.0000 | P_abs (kPa) | 98.5 | T_oil (^C) | 69.6 |

CO(gr/kW-hr) NOx(gr/kW-hr) HC(gr/kW-hr) CO2(gr/kW-hr)

CO(gr/hp-hr) NOx(gr/hp-hr) HC(gr/hp-hr) CO2(gr/hp-hr)

46.7 2.4 14.85 2242.84

48.3 1.8 11.08 1673.16

CO(gr/hr) NOx(gr/hr) HC(gr/hr) CO2(gr/hr)

31.2 1.1 7.16 1081.17

BSFC (gr/kW/hr): 1088.53 Fuel burned (%): 98.64

Dilution Factor 36.20 AFR: 14.00

Dilution Factor (EPA)35.11

[CO]/[CO2]: 0.0288

LIST OF REFERENCES

LIST OF REFERENCES

- 1) Blumberg, P and Kummer, J.T., "Prediction of NO Formation in Spark Ignited Engines - An Analysis of Methods of Control", Combustion Science and Technology, Volume 4, pp. 73-95, 1971.
- 2) Robinson, J.A., "Humidity Effects on Engine Nitric Oxide Emissions at Steady-State Conditions", SAE Paper 700467, 1970.
- 3) Sodre, J.R. and Yates, D.A., "Species and Time-Resolved Measurements of Exhaust Hydrocarbons from a SI Engine", SAE Paper 971016, 1997.
- 4) Donohue, J.A., Hardwick, G.C., Newhall, H.K., Sanvordenker, K.S. and Woelffer, N.C., "Small Engine Exhaust Emissions in the United States", SAE Paper 720198, 1972.
- 5) Mooney, J.J., Shinn Hwang, H., Daby, K.O. and Winberg, J.R., "Exhaust Emission Control of Small 4-Stroke Air Cooled Utility Engines an Initial R & D Report", SAE Paper 941807, 1994.
- 6) Eccleston, B.H. and Hurn, R.W., "Exhaust Emissions from Small, Utility, Internal Combustion Engines", SAE Paper 720197, 1972.
- 7) Brereton, G.J., DeAraujo, A. and Bertrand, E., "Effects of Ambient Conditions on the Emissions of a Small Carbureted Four-Stroke Engine", SAE Paper 961739, 1996.

- 8) Spindt, R.S., "Air-Fuel Ratios from Exhaust Gas Analysis", SAE Paper 650567, 1965.
- 9) Hare, C.T., Springer, K.J., Oliver, W.R. and Houtman, W.H., "Small Engine Emissions and Their Impact", SAE Paper 730859, 1973.
- 10) White, J.J., Carroll, J.N., Hare, C.T., and Lourenco, J.G., "Emission Control Strategies for Small Utility Engines", SAE Paper 911807, 1991.
- 11) Sun, X., Brereton, G., Morrison, K. and Patterson, D., "Emissions Analysis of Small Utility Engines", SAE 952080, 1995.
- 12) Sun, X., Assanis, D. and Brereton, G., "Assessment of Alternative Strategies for Reducing Hydrocarbon and Carbon Monoxide Emissions from Small Two-Stroke Engines"
- 13) Brereton, G.J., Morrison, K., Chishty, H.A., Schwartz, G. and Patterson, D.J., "Measured Emissions of Small Engines under Steady State and Transient Operation", SAE Paper 941806, 1994.
- 14) Reynolds, R.C., "STANJAN", a computer program used for analyzing combustion problems, Dept. of Mechanical Engineering, Stanford University
- 15) Woshni, G., "A Universally Applicable Equation for the Instantaneous Heat Transfer Coefficient in the Internal Combustion Engine", SAE Paper 670931, 1967.

- 16) Ramos, J.I., "Internal Combustion Engine Modeling", Hemisphere Publishing Corporation, 1989.
- 17) Taylor, C.F., "The Internal Combustion Engine in Theory and Practice", Volumes 1 and 2, M.I.T. Press, Revised Edition 1985.
- 18) Zeggeren, V., and Storey, S.H., "The Computation of Chemical Equilibria", Cambridge University Press, 1970.
- 19) Heywood, J.B., "Internal Combustion Engine Fundamentals", McGraw Hill Series in Mechanical Engineering, 1988.
- 20) Munson, B.R., Young, D.F. and Okiishi, T.H., "Fundamentals of Fluid Mechanics", John Wiley and Sons Publishing, 1990.
- 21) California Air Resources Board (CARB) homepage:
<http://arbis.arb.ca.gov/homepage.htm>.
- 22) "Test Procedure for Measurement of Gaseous Exhaust Emissions from Small Utility Engines", SAE J1088 Recommended Practice, 1983.
- 23) Sonntag, R.E., VanWylen, G.J., "Introduction to Thermodynamics", John Wiley and Sons, Inc., 1991.
- 24) Micro Motion Model RFT9739 Instruction Manual, 1992.

MICHIGAN STATE UNIV. LIBRARIES



31293017167382